https://doi.org/10.5194/egusphere-2026-3323
Preprint. Discussion started: 24 June 2026

Vegetation structure drives carbon dioxide and methane dynamics in adjacent boreal fen and bog ecosystems

Eyrún Gyða Gunnlaugsdóttir[1], Angelika Kübert[1], Xuefei Li[1], Timo Vesala[1,2], Aino Korrensalo[3,4], Elisa Männistö[3], Eeva-Stiina Tuittila[3], Pavel Alekseychik[5] and Ivan Mammarella[1]

[1]Institute for Atmospheric and Earth System Research (INAR)/Physics, Faculty of Science, University of Helsinki, Helsinki, Finland
[2]Institute for Atmospheric and Earth System Research (INAR)/Forest Sciences, Faculty of Agriculture and Forestry, University of Helsinki, Helsinki, Finland
[3]Peatland and soil ecology research group, School of Forest Sciences, University of Eastern Finland, P.O. Box 111, 8010 Joensuu, Finland
[4]Natural Resources Institute Finland (LUKE), Soil Ecosystems Group, Paavo Havaksen tie 3, FI-90570 Oulu
[5]Natural Resources Institute Finland (LUKE), Ecosystems and Modelling Group, Latokartanonkaari 9, FI-00790 Helsinki

Correspondence to: Eyrún Gyða Gunnlaugsdóttir (eyrun.gunnlaugsdottir@helsinki.fi)

Abstract. Boreal peatlands store substantial soil carbon and differ strongly in greenhouse gas exchange depending on factors such as hydrology and vegetation. Understanding these differences is increasingly important because many boreal peatlands are undergoing fen-to-bog transitions, potentially altering ecosystem carbon cycling and greenhouse gas exchange. We compared active-season (May–October) carbon dynamics between an oligotrophic sedge fen and an ombrotrophic patterned bog located 1.2 km apart within the Siikaneva wetland complex, southern Finland. We analysed fluxes of carbon dioxide (CO_2) and methane (CH_4) at diurnal, seasonal, and interannual scales, using eddy covariance measurements from 2011–2016. These fluxes were related to abiotic and biotic drivers, including soil temperature, photosynthetically active radiation, water table depth, and vascular plant leaf area index (LAI), with a focus on aerenchymatous LAI (LAI_{Aer}).

Across the six-year period both ecosystems acted as CO_2 sinks during the active-season and the fen was generally a stronger sink (mean±std NEE -80.8±42.1 g C m^{-2} $season^{-1}$) than the bog (-72.2±22.5 g C m^{-2} $season^{-1}$). The fen also exhibited higher gross primary production (GPP) and light-use efficiency, consistent with its higher total LAI, indicating vegetation structure and phenology as key drivers of the CO_2 sink difference under shared climate. CH_4 emissions were substantially higher at the fen (mean±std CH_4 10.8±2.3 g C m^{-2} $season^{-1}$) than the bog (7.9±1.4 g C m^{-2} $season^{-1}$). CH_4 fluxes scaled positively with total LAI and LAI_{Aer}, supporting the role of substrate supply and plant-mediated transport.

The contrasting carbon dynamics between these adjacent peatland types suggest that ongoing fen-to-bog transitions may alter active-season carbon exchange by reducing CO_2 uptake and CH_4 emissions as vegetation composition and hydrological conditions shift toward bog-like states. Our results additionally indicate greater temporal variability in carbon fluxes at the fen than the bog. These findings highlight the importance of representing vegetation composition and canopy development in peatland models, rather than relying solely on peatland type.

https://doi.org/10.5194/egusphere-2026-3323
Preprint. Discussion started: 24 June 2026

1 Introduction

Peatlands exchange large amounts of carbon (C) with the atmosphere through the uptake and emission of carbon dioxide (CO_2) and the release of methane (CH_4) (Saunois et al., 2025; Limpens et al., 2008). Peatlands in the boreal and subarctic regions are of particular interest because, despite covering only approximately 3% of the global land surface (Rydin et al., 2013), they represent one of the largest terrestrial carbon reservoirs and play a significant role in carbon cycling (Yu, 2012; Gorham, 1991). Carbon accumulation in peatlands results from slower decomposition than photosynthetic carbon uptake. Water table depth (WTD) strongly influences oxygen availability in peat soils. When the WTD is close to the surface, oxygen diffusion into the peat profile is limited, creating anoxic conditions that slow decomposition, thereby promoting long-term C accumulation (Blodau et al., 2004). Fresh root litter and exudates provide key substrates for methanogenic microbes, and a substantial proportion of CH_4 production originates from this labile organic matter rather than from older, more recalcitrant peat (Koelbener et al., 2010). Consequently, CH_4 fluxes are strongly and positively correlated with CO_2 uptake (Rinne et al., 2018). Boreal peatlands are a major natural source of atmospheric CH_4, contributing approximately 12% of global CH_4 emissions (Gorham, 1991; Wuebbles and Hayhoe, 2002), while wetlands as a whole account for about 24% of the global CH_4 emission budget (Saunois et al., 2025). Because peatland carbon exchange is tightly linked to hydrology and vegetation, understanding how peatlands with contrasting ecosystem characteristics respond to environmental variability is essential for predicting their carbon-cycle feedbacks under global change.

Bogs and fens are the two principal types of boreal peatlands, distinguished by their hydrology, nutrient status, and vegetation composition. Bogs are ombrotrophic systems that receive water inputs exclusively from precipitation, making them nutrient-poor. Fens, by contrast, are minerotrophic; in addition to rainfall, they are fed by mineral-rich groundwater, resulting in higher nutrient availability and typically higher pH than in bogs. These contrasting environmental conditions shape their plant communities. Bogs are typically dominated by *Sphagnum* mosses and are often characterised by a microtopographical variation between dry hummocks dominated by ericaceous shrubs and sedge-dominated wet hollows. Fens have typically spatially more homogeneous and sedge-dominated flora, at times *Sphagnum* mosses being accompanied by brown mosses (Charman, 2002). These differences between fens and bogs strongly influence ecosystem functioning, including CH_4 dynamics and net ecosystem exchange (NEE) of CO_2 (e.g. Limpens et al., 2008; Rinne et al., 2020; Riutta et al., 2007). Because bogs and fens differ in key ecological characteristics, they are likely to respond differently to environmental variability and long-term change. This makes it essential to understand how CO_2 sequestration and CH_4 emissions vary between these peatland types.

Fens can transition into bogs through time, as plant litter accumulates and thickens the peat layer, progressively reducing the influence of mineral-rich groundwater and shifting the system toward increasingly ombrotrophic conditions. This successional process, known as a fen-bog transition (FBT), may occur during natural peatland development but can also be accelerated by changes in catchment hydrology or climate warming (Kolari et al., 2022; Kolari and Tahvanainen, 2023; Tahvanainen, 2011). As FBT progresses, vegetation composition shifts toward *Sphagnum* dominance, while sedges and other fen-characteristic plant communities decline, with consequences for peatland carbon cycling and greenhouse gas exchange. Consistent with these

https://doi.org/10.5194/egusphere-2026-3323
Preprint. Discussion started: 24 June 2026

vegetation and hydrological changes, FBT has been shown to alter peatland carbon cycle feedbacks, for example by increasing carbon sequestration (Loisel and Yu, 2013) and reducing CH_4 emissions (Zhang et al., 2021). Seasonal CO_2 exchange in boreal peatlands is largely controlled by plant community composition and phenology, as different functional groups peak in productivity at different times during the growing season. Carbon exchange in fens is generally more temporally variable than in bogs, as vascular plant productivity drives pronounced seasonal fluctuations, whereas *Sphagnum* dominated bogs typically exhibit more stable CO_2 dynamics (Leppälä et al., 2009). This stability can be linked to the functional role of *Sphagnum* species which suppresses decomposition by acidifying the peat environment, enhancing mineral soil organic carbon interactions, and inhibiting microbial activity under aerobic conditions. As a result, *Sphagnum*-dominated systems tend to exhibit lower decomposition rates and greater carbon stability (Zhao et al., 2026). Future changes in vegetation structure and composition driven by FBT may therefore alter peatland ecosystem functioning and their response to climatic variability. The FBT can be accelerated under climate warming (Kolari and Tahvanainen, 2023; Tahvanainen, 2011), highlighting the need to better understand how shifts from fen to bog communities influence contrasting greenhouse gas emission patterns.

Fens generally exhibit higher CH_4 emissions than bogs (Juottonen et al., 2005; Saarnio et al., 2009; Turetsky et al., 2014; Webster et al., 2018), reflecting differences in key environmental controls. One important factor is pH: bogs are typically more acidic, whereas fens have higher, more neutral pH conditions. CH_4 production in peatlands often increases with pH due to enhanced methanogenic activity under less acidic conditions, with maximum production reported at approximately pH 5.5 (Kusin et al., 2025; Ye et al., 2012). Vegetation is another major control on CH_4 emissions. Methanogenesis is strongly influenced by the availability of labile carbon substrates derived from fresh plant litter and root exudates (Koelbener et al., 2010). Plant community composition is also closely linked with CH_4 emissions, with higher emissions observed in sedge-dominated fens where vascular plant biomass and associated carbon inputs are greater (Abdalla et al., 2016; Järvi-Laturi et al., 2025). Aerenchymatous plants both provide labile substrates and facilitate CH_4 transport from peat to the atmosphere via aerenchyma (Jentzsch et al., 2024; Koelbener et al., 2010; Korrensalo et al., 2022; Leppälä et al., 2011), a specialised plant tissue characterised by extensive intercellular air-filled spaces or channels in roots, stems, and/or leaves, which facilitate internal gas transport between aerial and submerged parts. These spaces reduce resistance to diffusion and help plants tolerate hypoxic or anoxic conditions by enabling oxygen diffusion to roots (Evans, 2004). The aerenchyma tissue also provides pathways for CH_4 to bypass the oxic layers, where oxidation could otherwise reduce the CH_4 emission (van den Berg et al., 2020; Turner et al., 2020).

Vegetation mediated processes may also influence the temporal coupling between CO_2 uptake and CH_4 emissions. CH_4 fluxes can exhibit time lags and hysteretic relationships relative to gross primary productivity (GPP) and temperature (Chang et al., 2020; Kettunen et al., 2000; Rinne et al., 2018). These hysteretic relationships likely reflect delayed belowground transfer of assimilated carbon, microbial processing, and transport through peat and plant tissues, with fens often showing more pronounced hysteresis than bogs (Chang et al., 2021). These dynamics may contribute to differences in temporal CH_4 variability between fen and bog ecosystems.

https://doi.org/10.5194/egusphere-2026-3323
Preprint. Discussion started: 24 June 2026

Currently, there is not a clear consensus regarding whether fens or bogs function as stronger CO_2 sinks. While many studies have suggested that fens are weaker CO_2 sinks than bogs (Leppälä et al., 2009; Turunen et al., 2002; Webster et al., 2018), others have reported fens to be a bigger sink of CO_2 (Bubier et al., 1998; Humphreys et al., 2006; Sulman et al., 2010). The contrasting results of these studies indicate that peatland carbon dynamics are strongly influenced by local ecosystem characteristics, such as vegetation and hydrology. Paired measurements from adjacent peatland ecosystems experiencing similar climatic conditions provide a valuable opportunity to isolate the role of ecosystem characteristics in controlling carbon exchange. However, direct comparisons of carbon flux dynamics between adjacent fen and bog ecosystems exposed to similar climatic conditions remain limited.

The aim of this study is to examine differences in CO_2 and CH_4 flux dynamics between adjacent boreal fen and bog ecosystems, which are therefore exposed to similar climatic conditions. Specifically, we investigated whether these fluxes differed at seasonal, annual, and diurnal scales within the active-season (May–Oct), and which abiotic and biotic variables were the main drivers of these differences. We hypothesise that the fen exhibits a (i) smaller active-season CO_2 net uptake, (ii) higher CH_4 emissions, and (iii) greater temporal variability in CO_2 and CH_4 fluxes than the adjacent bog.

2 Materials and Methods

2.1 Measurement Sites

Siikaneva wetland complex is located in Southern Finland (61°50’ N, 24°12’ E, 162 m a.s.l.) and comprises a 12 km^2 boreal peatland, where the peat depths range from 2–6 m (Mathijssen et al., 2016). The complex includes both minerotrophic aapa mire areas and ombrotrophic bog areas. Our study sites were located 1.2 km from each other (Fig. 1) within an oligotrophic sedge fen and an ombrotrophic patterned bog.

The climate is boreal and with an annual temperature of 3.3°C and rainfall of 710 mm for the period 1971–2000 (Drebs, 2002). Snow cover typically persists from November–December until April–May (Rinne et al., 2018). We analysed data obtained simultaneously from both sites during the active seasons (May–October) of 2011–2016.

Figure 1: Aerial photo from Siikaneva showing locations of Eddy covariance flux measurement towers in Siikaneva fen and bog sites. Background imagery from Esri World Imagery | Powered by Esri, visualised in QGIS v3.36.2

https://doi.org/10.5194/egusphere-2026-3323
Preprint. Discussion started: 24 June 2026

The Siikaneva fen site has a relatively flat topography and a homogeneous surface structure with minimal hollow, lawn, and hummock patterning. The vegetation is dominated by peat mosses (*Sphagnum balticum* (Russow) C.E.O. Jensen, *Sphagnum majus* (Russow) C.E.O. Jensen, *Sphagnum papillosum* Lindb.), sedges (*Carex rostrata* Stokes, *Carex limosa* L., *Eriophorum vaginatum* L.), and Rannoch rush (*Scheuchzeria palustris* L.). A more detailed description of the site's vegetation composition is provided by Riutta et al. (2007) and Laine et al. (2012).

The Siikaneva bog site is characterised by distinct microtopography and heterogeneous vegetation. Lower lying areas within the site consist of hollows and lawns, moss free mud bottoms, and open-water ponds, with pond depths ranging from 0 to 2 m. The site exhibits considerable spatial variability in vegetation composition and WTD, resulting in a highly heterogeneous ecosystem (Korrensalo et al., 2018). A clear microtopographic gradient is apparent with elevated hummocks dominated by dwarf shrubs, *Sphagnum* species (*S. rubellum* (Ehrh.) Hedw., *S. papillosum, S. fuscum* (Schimp.) H.Klinggr.), and occasional Scots pine (*Pinus sylvestris* L.), while hollows support vegetation more typical of ombrotrophic conditions, including sedges and species such as *Rhynchospora alba* (L.) Vahl. Other species at the bog site include *Andromeda polifolia* L., *Calluna vulgaris* (L.) Hull, and *Rubus chamaemorus* L. Some areas contain open-water surfaces or naturally bare peat with only sparse vegetation cover (mud bottoms) (Korrensalo et al., 2022). The bog site is relatively wet and with less shrubs or small trees when compared with many other previously studied bogs, the shrub dominated hummocks are a minority (Korpela et al., 2020). Further details on the vegetation composition and microform structure are available in Korrensalo et al. (2016, 2017).

2.2 Flux measurements

The eddy covariance (EC) method (e.g. Aubinet et al., 2012) was used to measure CO_2 and CH_4 fluxes. Measurements at the bog site were conducted during 2011–2016. Electricity at the site was provided by solar panels, therefore data were available only during the active-season. The bog EC system was mounted at 2.4 m height above the ground and consisted of a METEK USA-1 three-dimensional sonic anemometer (METEK GmbH, Germany) for measuring wind velocity components and the sonic temperature, a LI-7700 open-path CH_4 analyser, and a LI-7200 enclosed-path CO_2 and H_2O analyser (LI-COR Biosciences, USA). Detailed descriptions of the EC instrumentations and setup is available in Alekseychik et al. (2021).

Measurements at the fen site began in 2004, but only data from 2011–2016 were used in this study to match the period available from the bog site. The EC system, located at 2.75 m height above the ground, included an ultrasonic anemometer (METEK USA-1 GmbH, Germany) to measure the three wind velocity components and the sonic temperature, closed path gas analysers to measure CH_4 and H_2O concentrations (Picarro Inc, USA and Los Gatos Research, USA) and a LI-7000 infrared gas analyser (LI-COR Biosciences, USA) to measure CO_2 and H_2O concentrations. Detailed descriptions of the EC instrumentations and setup are given in Rinne et al. (2018).

2.2.1 Flux processing and gapfilling

EC data processing and flux calculation were done by using EddyUH software (Mammarella et al., 2016), following standard methods and processing pipelines. CO_2 and CH_4 flux data were quality flagged according to the Mauder and Foken (2004)

https://doi.org/10.5194/egusphere-2026-3323
Preprint. Discussion started: 24 June 2026

system, with three quality flag classes and only data with quality flags 0 and 1 were used. Fluxes were also storage corrected and filtered for low turbulence conditions (friction velocity lower than 0.1 m/s). Data availability at both sites for each year is presented in Appendix A.

Both CO_2 and CH_4 fluxes were gapfilled using XGBoost machine learning, as described in Vekuri et al. (Vekuri et al., 2023). Environmental variables for the training of the method for gapfilling of CO_2 were PAR, global radiation, soil temperature at 5 cm depth, air temperature, and WTD. The environmental variables used for the gapfilling of CH_4 were soil temperature at 5 cm depth and WTD. The gapfilled flux data were only used for estimating the active-season carbon balance; all other analyses were based on measured values.

Finally, we partitioned NEE into Terrestrial Ecosystem Respiration (TER) and GPP by using nighttime based flux partitioning approach (Reichstein et al., 2005), where TER was estimated from nighttime NEE and extrapolated to daytime. GPP was then calculated as TER minus NEE.

2.3 Ancillary measurements

Ancillary measurements at both sites included air temperature, relative humidity, soil temperature, WTD, Leaf area index (LAI) and photosynthetically active radiation (PAR).

Air temperature and relative humidity were measured by Campbell CS215 sensor at the bog site and Rotronic HC2 sensor at the fen site. During the study period, WTD was measured using a PDCR1830 pressure transducer (DRUCK & TEMPERATUR Leitenberger GmbH, GERMANY) at the fen and a CS 451 pressure transducer (Campbell Scientific, UK) at the bog.

Soil temperature was measured at lawn microsites using Campbell 107 thermistors installed at both the fen and bog sites at several depths (5, 20, and 35 cm), within the footprint of the EC tower.

LAI data were obtained from manual measurements conducted during 2014–2016 at the fen and 2012–2016 at the bog, for further information on the method of manual measurements for the fen in Männistö et al. (2023) and the bog in Korrensalo et al. (2018). For our study, LAI data were separated into total vascular plant LAI (LAI_{Tot}) and the LAI of aerenchymatous species (LAI_{Aer}), which facilitate gas transport. The following species were classified as aerenchymatous in both sites; *Carex* spp., *Eriophorum vaginatum*, *Scheuchzeria palustris* and *Rhynchospora alba*.

PAR was measured at the fen site using a Li-190R quantum sensor (LI-COR, Inc., USA). PAR from the fen site was used for both ecosystems due to better data availability than at the bog site. In 2011–2012 PAR measurements at the fen site were affected by instrument failure, and missing values from that time or other gaps in the data were filled using PAR data from the nearby Hyytiälä forest research station.

Vapor pressure deficit (VPD) was calculated from air temperature (T, °C) and relative humidity (RH, %) following the Tetens equation. First, saturation vapor pressure (SVP, Pa) was computed as:

$$SVP = 0.611 \times exp\left(\frac{(17.2694 \times T)}{(T + 237.3)}\right) \quad (1)$$

VPD was obtained as the difference between saturation and actual vapor pressure:

https://doi.org/10.5194/egusphere-2026-3323
Preprint. Discussion started: 24 June 2026

$$VPD = SVP \times \left(1 - \frac{RH}{100}\right) \quad (2)$$

2.4 Temporal variability of CO_2 and CH_4 fluxes

2.4.1 Diurnal variability

Previous studies at Siikaneva fen have shown that CH_4 fluxes do not exhibit a consistent diurnal cycle when examined over July–September (Rinne et al., 2007) or the full year (Rinne et al., 2018). To investigate whether diurnal patterns might emerge over shorter time scales, we analysed the data on a monthly basis (May–October).

For each month, 30 min flux observations were grouped by hour of day, and mean ± standard error were calculated to provide an average representation of daily patterns. Diurnal variability was assessed using a Kruskal-Wallis test across hourly bins. We further fitted a 24 h cosinor model to hourly mean fluxes, and the joint significance of sine and cosine terms was used to test for rhythmicity.

To quantify differences between sites, hourly median fluxes were compared between fen and bog, and differences in the absolute magnitudes of NEE and CH_4 fluxes were calculated for each hour. Daytime (06:00–18:00) and nighttime (18:00–06:00) periods were defined, and the maximum and minimum differences within each period were identified for each month.

2.4.2 Seasonal variability

To explore the main patterns in ecosystem carbon fluxes at different seasonal stages, between the two peatland site types and in relation to their environmental controls, we performed a principal component analysis (PCA) using R (version 4.3.2) with the vegan package (Oksanen et al., 2015). The PCA was conducted on measured non-gapfilled daily flux variables (CH_4, NEE, GPP, and TER).

Environmental variables (soil temperature at 5, 20, and 35 cm depth, PAR, air temperature, VPD, WTD, LAI_{Tot} and LAI_{Aer}) were fitted passively onto the ordination using the envfit function inside the vegan package (Oksanen et al., 2015). The significance of fitted vectors was assessed using 999 permutations, and only variables with $p \leq 0.05$ were retained. Observations were grouped by ecosystem type (fen and bog) and season (early, mid, and late active-season). Group centroids were calculated as the mean ordination position for each site–season combination, and group dispersion was visualised using 68% confidence ellipses based on a multivariate t distribution.

Availability of LAI data from the fen site restricted the PCA to the years 2014-2016. To assess the influence of this limitation, we repeated the analysis excluding LAI, thereby including the full 2011–2016 dataset. The overall structure of the ordination and relationships among flux variables remained consistent between analyses, and we thus display and base our interpretations on the analysis including LAI.

For visualisation, flux (species) scores were rescaled relative to the range of site scores to improve comparability of vector lengths while preserving their direction in ordination space. Environmental vectors were plotted according to their fitted

https://doi.org/10.5194/egusphere-2026-3323
Preprint. Discussion started: 24 June 2026

directions. The proportion of variance explained by each principal component was calculated from eigenvalues and is reported on the corresponding axes.

2.4.3 Interannual variability

To examine interannual variability in active-season CO_2 exchange, cumulative gapfilled NEE was calculated separately for the fen and bog ecosystems for each study year. It was integrated over the active-season and expressed as cumulative carbon balance in grams of carbon per square metre. The year 2011 was excluded from the carbon balance estimates for the bog, as measurements commenced in July 2011 and there was a lack of soil temperature data at 5cm depth, resulting in insufficient data for reliable gapfilling. Cumulative NEE was then plotted as a function of day of year for each year, allowing differences in the seasonal development, timing, and final magnitude of carbon uptake to be compared among years and between ecosystems.

2.5 Driver analysis

2.5.1 Soil temperature

CH_4 flux (Kübert et al., 2026; Rinne et al., 2018; Kim et al., 1999) and TER (Chen et al., 2022; Bond-Lamberty and Thomson, 2010) have been shown to have an exponential relationship with soil temperature. Therefore, the temperature dependence of CH_4 flux and nighttime NEE was analysed for the active-season, with nighttime conditions of NEE defined as PAR <10 µmol m^{-2} s^{-1}. The response to soil temperature measured at 5, 20, and 35 cm depth was visualised using the exponential model described in Eq. (3), where only positive flux values were included in model fitting to ensure compatibility with the exponential formulation.

$$y = ae^{bx} \quad (3)$$

where y represents the flux, x the soil temperature, a the fitted intercept corresponding to the baseline flux at $x = 0$, and b the apparent response coefficient. Model parameters were estimated using non-linear least squares regression.

The coefficient of determination (R^2) was used to assess the model fit, and statistical significance was evaluated from the linear regression of ln(y) against temperature. Temperature sensitivity was further expressed using the Q_{10} coefficient, which describes the multiplicative change in flux associated with a 10 °C increase in temperature, calculated as:

$$Q_{10} = e^{10b} \quad (4)$$

2.5.2 Vegetation

To assess how vascular plant development influenced CH_4 fluxes, we quantified relationships between CH_4 exchange and LAI. For each combination of ecosystem type (fen/bog) and LAI metric (LAI_{Tot} / LAI_{Aer}), we fitted a linear regression of the form

$$y = \beta_0 + \beta_1 x \quad (5)$$

https://doi.org/10.5194/egusphere-2026-3323
Preprint. Discussion started: 24 June 2026

where y represents CH_4 flux (µmol m^{-2} s^{-1}) and x the LAI (m^2 m^{-2}). We reported the slope, intercept, coefficient of determination (R^2), and p-value for each relationship.

In order to obtain continuous seasonal LAI trajectories, we fitted low-order polynomials (3 degree) to each year of observations separately. The resulting per-year fitted series was used for visualisation and to gapfill missing observations of daily values for further analysis. Linear mixed-effects models were used to evaluate the relationship between LAI and ecosystem fluxes. Four models were fitted with either CH_4 flux or GPP as the response variable and either total LAI_{Tot} or LAI_{Aer} as the predictor. Site type (fen vs bog), LAI, and their interaction were included as fixed effects to test whether the slope of the relationship differed between site types. Seasonal periods (May–June, July–August, September–October) were included as a random intercept.

2.5.3 Seasonal response of CH_4

Seasonal differences in the relationships between CH_4 fluxes, soil temperature at 5 cm depth, and GPP were examined using exponential response functions. Relationships between CH_4 fluxes and GPP were analysed to assess potential links between vegetation productivity and CH_4 emissions during the active season. To facilitate seasonal comparison, the data were divided into two periods (May–July & August–October). Daily CH_4 fluxes were plotted against soil temperature at 5 cm depth and GPP separately for the fen and bog ecosystems. Exponential relationships between CH_4 fluxes and explanatory variables were fitted separately for each ecosystem and seasonal period using the model described in Eq. (3), allowing seasonal differences in CH_4 responses to temperature and productivity to be quantified.

2.5.4 Seasonal response of photosynthetic parameters

To quantify the photosynthetic response to light availability, we constructed light response curves for GPP across the measurement period. PAR from the fen site was used as the incoming light metric, and air temperature from each site included as a modifying factor. We only used PAR values > 10 µmol m^{-2} s^{-1}, to remove near dark conditions. Each site was fitted independently, and the resulting curves were evaluated across 0–2000 µmol m^{-2} s^{-1} PAR, grouped into 250 µmol m^{-2} s^{-1} bins. Mean GPP and standard deviation were calculated and plotted as error bars on top of the fitted line.

Light use efficiency (LUE) was calculated as the ratio of GPP (µmol CO_2 m^{-2} s^{-1}) to PAR (µmol photons m^{-2} s^{-1}) during daylight periods. Daily LUE was computed from summed daily GPP and PAR and subsequently averaged by month. Maximum gross photosynthetic capacity (P_{max}) was derived from the fitted light response curves. For each ecosystem and for each year-month combination during the active-season, the light response model was fitted to GPP observations using PAR values > 10 µmol m^{-2} s^{-1}. The fitted model was then evaluated across a PAR range of 0–2000 µmol m^{-2} s^{-1}, and P_{max} was defined as the maximum value of the modelled photosynthetic response within this range. Monthly mean P_{max} values were calculated separately for the fen and bog sites, and variability was expressed as the standard error of the mean across years.

https://doi.org/10.5194/egusphere-2026-3323
Preprint. Discussion started: 24 June 2026

2.5.5 Hysteresis and lag time correlation

Monthly hysteresis relationships between CH_4 flux and GPP were analysed using monthly mean values derived from measured daily flux datasets for fen and bog sites separately. Analyses focused on the years 2012, 2014, and 2016, due to data availability. Monthly hysteresis plots were constructed by plotting monthly mean CH_4 fluxes against monthly mean GPP, with months connected sequentially within each year to illustrate seasonal trajectories. For visualisation continuity, missing bog monthly values were linearly interpolated for line segments only (July 2012, explicitly), while markers and month labels were shown exclusively for observed data points.

To assess the temporal coupling between CH_4 fluxes and GPP, a lag-correlation analysis was performed using daily mean values. Pearson correlation coefficients were calculated between absolute daily CH_4 fluxes and lagged absolute daily GPP values over lag periods ranging from 0 to 50 days, where positive lags indicate GPP leading CH_4 flux responses. Correlations were computed after removal of missing values independently for each lag step. The resulting lag-response curves were used to identify temporal offsets associated with the strongest CH_4–GPP coupling.

3 Results

3.1 Abiotic and biotic conditions

WTD was strongly correlated between the two sites (Pearson's r = 0.88) but fluctuated more in the fen than in the bog (Fig. 2a). The fen generally exhibited lower WTD during the middle of the active-season, whereas it remained relatively stable at the bog. In the fen, WTD ranged from a maximum of 8.2 cm (2016) to a minimum of -37.2 cm (2011), with a mean of -7.4 cm (±8.3). In the bog, WTD ranged from 2.8 cm (2012) to -17.4 cm (2014), with a mean of -10.4 cm (±3.0). Because only one WTD logger was installed at each site, mean WTD reflects local conditions rather than overall site wetness.

Air temperature was highly consistent across the sites (r = 0.98) (Fig. 2b). Soil temperature was also highly correlated between sites (r = 0.94), with the fen having soil temperatures at 35 cm depth ranging from 3.1 to 16.4 °C, while at the bog it ranged from 1.4 to 16.6 °C (Fig. 2c). Weekly mean PAR values ranged from 10.2 to 696.1 µmol m^{-2} s^{-1} (Fig. 2d).

Compared to the bog, the fen had consistently higher LAI_{Tot} and LAI_{Aer} (Fig. 2e-f). The maximum daily LAI_{Tot} reached 0.68 m^2 m^{-2} at the fen, compared with 0.49 m^2 m^{-2} at the bog, whereas maximum LAI_{Aer} values were 0.50 m^2 m^{-2} at the fen and 0.26 m^2 m^{-2} at the bog. Across monthly averages, mean LAI_{Tot} and LAI_{Aer} were significantly higher in the fen than in the bog (Wilcoxon signed-rank test, $p < 0.001$ for both variables). On average, LAI_{Tot} was 55% higher and LAI_{Aer} was 138% higher in the fen relative to the bog.

https://doi.org/10.5194/egusphere-2026-3323
Preprint. Discussion started: 24 June 2026

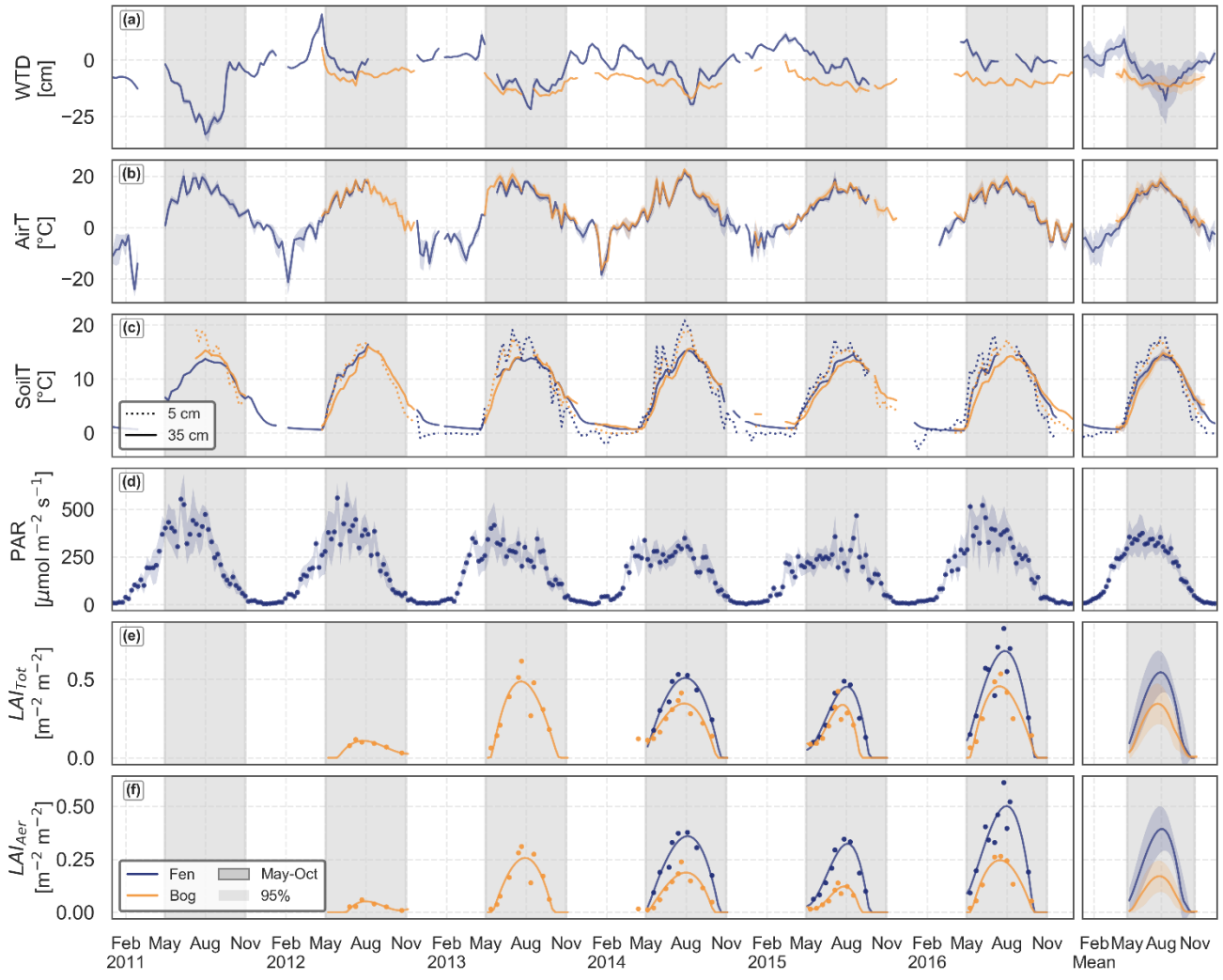

Figure 2: Weekly means from the years 2011 – 2016 of potential drivers of CO_2 and CH_4 fluxes from fen (blue) and bog (orange), with shaded 95% confidence interval. The active season (May–Oct), our study period, is shaded grey. WTD, water table depth; AirT, air temperature; SoilT, soil temperature (5 and 35 cm depth); PAR, photosynthetically active radiation; LAI_{Tot}, total leaf area index; LAI_{Aer}, aerenchymatous leaf area index. For LAI, points represent measurements and lines the polynomial fit.

3.2 Temporal variability in CO_2 and CH_4 fluxes

The bog had a narrower range of weekly mean values for all studied carbon flux variables. Weekly mean CH_4 fluxes ranged from 0.014 to 0.097 µmol m^{-2} s^{-1} at the bog and from 0.003 to 0.153 µmol m^{-2} s^{-1} at the fen. At both sites the minimum CH_4 flux occurred in October 2014, whereas maximum fluxes were observed in July 2014 (Fig. 3a).

Weekly mean NEE ranged from -2.20 to 0.19 µmol m^{-2} s^{-1} in the bog and from -3.40 to 0.47 µmol m^{-2} s^{-1} in the fen. The strongest CO_2 uptake (minimum weekly mean NEE) occurred in July at both sites, in 2013 at the fen and 2014 at the bog, while the highest NEE values were recorded in October (2016 at the fen and 2012 at the bog; Fig. 3b).

https://doi.org/10.5194/egusphere-2026-3323
Preprint. Discussion started: 24 June 2026

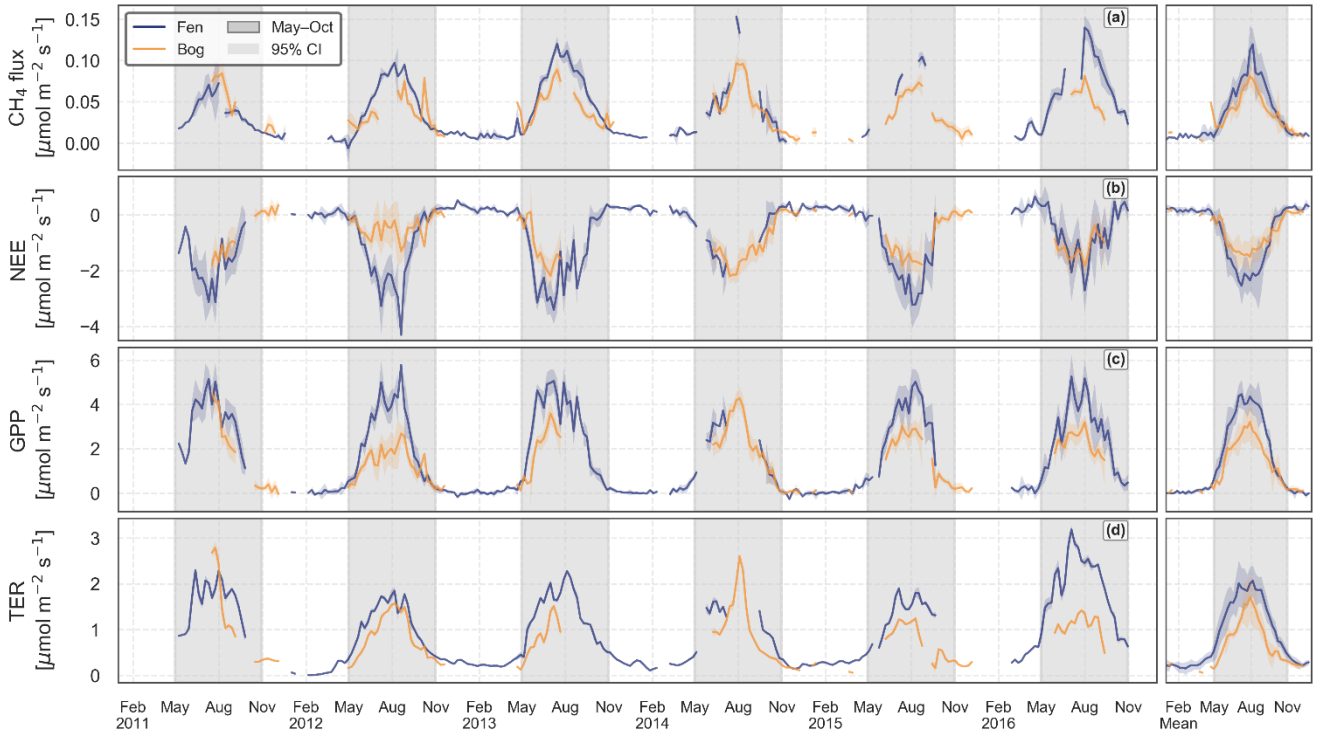

Figure 3: Weekly means of carbon flux at the fen (blue) and bog (orange) during 2011–2016. Shaded areas indicate the 95% confidence interval, and the active season (May-Oct), our study period, is shaded in grey. Mean for all years can be seen on the far right. CH_4, methane flux; NEE, net ecosystem exchange; GPP, gross primary production; TER, total ecosystem respiration.

Weekly mean GPP ranged from 0.05 to 5.25 µmol m^{-2} s^{-1} in the fen and from 0.10 to 4.49 µmol m^{-2} s^{-1} in the bog. Minimum values at both sites occurred in late October 2014, whereas maximum GPP was observed in July at both sites, in 2011 at the bog and 2016 at the fen (Fig. 3c).

TER showed a similar seasonal range, varying from 0.37 to 3.19 µmol m^{-2} s^{-1} at the fen and from 0.16 to 2.79 µmol m^{-2} s^{-1} at the bog. Maximum TER occurred concurrently with maximum GPP at both sites, July 2011 at the bog and July 2016 at the fen, whereas the minimum TER occurred in September 2015 in the bog and late October 2014 at the fen (Fig. 3d).

When averaged across years, both sites showed similar seasonal timing of CH_4 fluxes, with maxima in late July. Minima occurred in late October at the fen and in mid-October at the bog. NEE followed a similar seasonal trajectory, with strongest CO_2 uptake (most negative values) occurring in July, approximately one week earlier at the fen than at the bog, while peak emissions (most positive values) occurred in October at both sites, earlier at the fen and later at the bog.

GPP peaked in July at both sites, with the peak occurring about two weeks later at the bog than at the fen. TER exhibited a similar seasonal pattern, also peaking in July but happening approximately three weeks later at the bog relative to the fen.

https://doi.org/10.5194/egusphere-2026-3323
Preprint. Discussion started: 24 June 2026

3.2.1 Diurnal variation

NEE displayed strong and consistent diurnal cycles throughout the active-season (Fig. 4). Both the fen and bog sites showed highly significant differences among hours in every month from May to October ($p < 0.001$) and cosinor analysis confirmed a robust 24-hour periodicity. Amplitudes were highest during mid active-season (Jul–Aug), when photosynthetic activity was maximal. The NEE at the fen had a more pronounced diurnal amplitude than at the bog, acting as a stronger CO_2 sink during the day, but also releasing more CO_2 at night. Differences between sites generally scaled with flux magnitude. The maximum relative difference between sites in median daytime (06:00–18:00) NEE occurred in July (-3.76 µmol m^{-2} s^{-1} at the fen and -2.25 µmol m^{-2} s^{-1} at the bog), while the maximum nighttime (18:00–06:00) difference occurred in August (2.51 µmol m^{-2} s^{-1} at the fen and 0.98 µmol m^{-2} s^{-1} at the bog). Consistently, the smallest differences were observed in October for daytime (0.12 µmol m^{-2} s^{-1} at the fen and -0.002 µmol m^{-2} s^{-1} at the bog) and nighttime (0.43 µmol m^{-2} s^{-1} at the fen and 0.28 µmol m^{-2} s^{-1} at the bog).

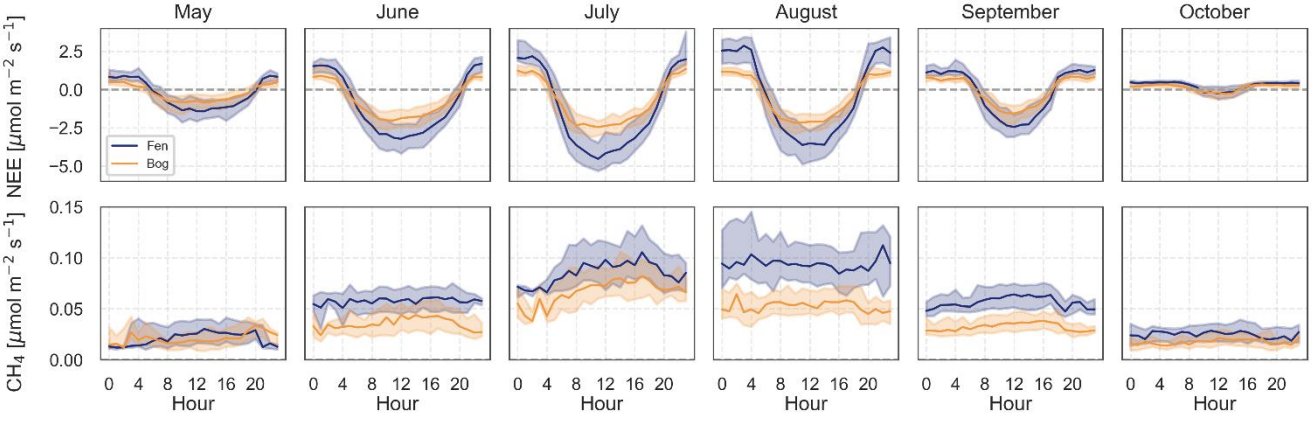

Figure 4: Monthly diurnal courses simultaneous measurements of net ecosystem exchange (NEE) and methane flux (CH_4) at the fen (blue) and bog (orange). Lines show medians and shaded areas the interquartile range (2011–2016). Hours are in UTC+2.

CH_4 fluxes showed weaker and less consistent diurnal variability than NEE for both sites (Fig. 4). At the bog site, significant diurnal cycles were observed in all months ($p < 0.05$), and cosinor models indicated periodicity from May through October. Median nighttime fluxes ranged from a minimum in May (0.01 µmol m^{-2} s^{-1} at the fen and 0.02 µmol m^{-2} s^{-1} at the bog) to a maximum at the fen in August (0.09 µmol m^{-2} s^{-1}) and at the bog in July (0.06 µmol m^{-2} s^{-1}). During daytime, the CH_4 median fluxes were highest at the fen in July and August (0.09 µmol m^{-2} s^{-1}) and at the bog in July (0.07 µmol m^{-2} s^{-1}). The daytime median CH_4 values reached a minimum in May (0.02 µmol m^{-2} s^{-1} at both sites). The fen CH_4 fluxes were on average higher than the bog fluxes both for daytime and nighttime, and they did not show a statistically significant diurnal pattern, except in May and July. The largest differences between sites were observed in August both for daytime (at the fen 0.09 µmol m^{-2} s^{-1} and 0.06 µmol m^{-2} s^{-1} at the bog) and nighttime (0.09 µmol m^{-2} s^{-1} at the fen and 0.05 µmol m^{-2} s^{-1} at the bog). The smallest daytime difference was in May (0.025 µmol m^{-2} s^{-1} at the fen and 0.019 µmol m^{-2} s^{-1} at the bog), while the smallest nighttime difference was in October (0.027 µmol m^{-2} s^{-1} at the fen and 0.019 µmol m^{-2} s^{-1} at the bog).

https://doi.org/10.5194/egusphere-2026-3323
Preprint. Discussion started: 24 June 2026

3.2.2 Seasonal variation

The largest variation in the daily C flux values was found between the stages of the active-season, and in both sites, mid-season (Jul-Aug) had the highest daily fluxes of GPP, TER and CH_4 and strongest CO_2 sink (most negative NEE fluxes) (Fig. 5). In the principal component analysis (PCA) the first axis (PC1, eigenvalue = 0.728) separated the daily C flux values by season, whereas the second axis (PC2, eigenvalue = 0.199) distinguished between ecosystems and their within-season variability. The C fluxes of the fen site had higher within-season variability than at the bog site, as displayed by the larger ellipses around the fen centroids along both gradients. Between- and within-season variability in GPP and NEE were more pronounced in the fen than in the bog, as reflected by greater separation of its centroids along the corresponding environmental arrows.

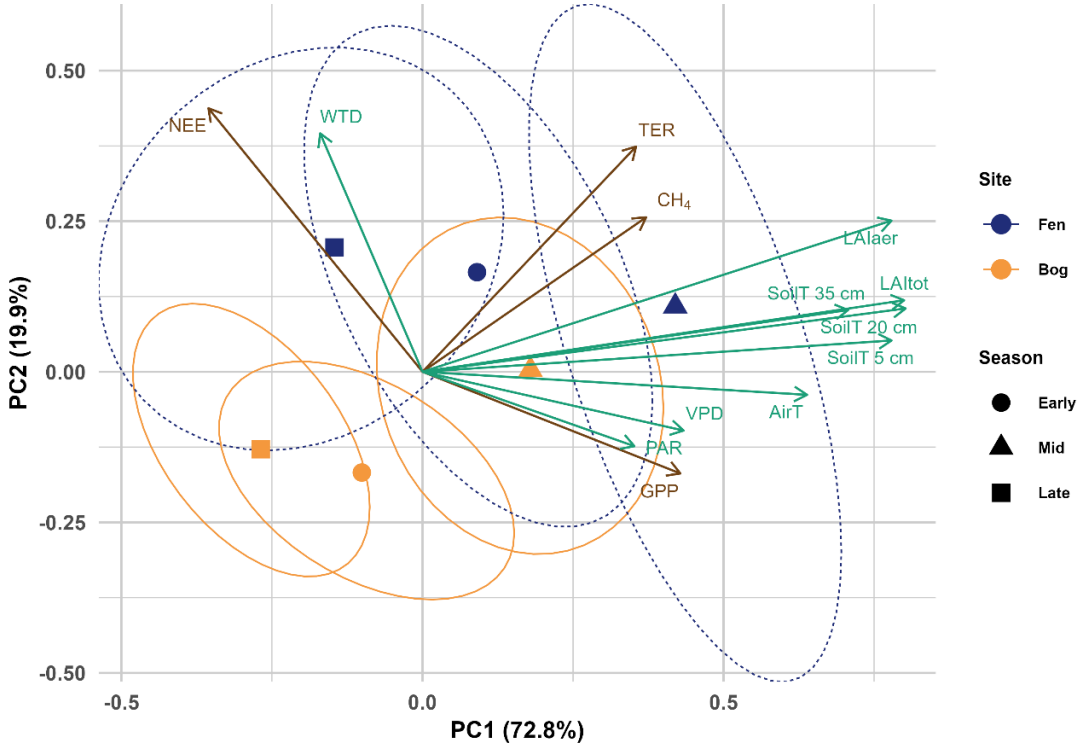

Figure 5: Principal component analysis (PCA) of Carbon fluxes and environmental variables in the fen and bog sites. The first two axes explain 72.8% (PC1) and 19.9% (PC2) of the total variance. Points represent site × season centroids (Early: May–Jun, Mid: Jul–Aug, Late: Sep–Oct), and ellipses indicate the 68% confidence intervals for each site–season grouping. Arrows show the direction and relative strength of correlations for measured fluxes (brown) and environmental variables (green). LAI data from the fen was only available from 2014–2016, therefore the PCA is limited to those years.

https://doi.org/10.5194/egusphere-2026-3323
Preprint. Discussion started: 24 June 2026

3.2.3 Interannual variation

As shown in Fig. 6 and Table 1, CO_2 exchange at the fen exhibited larger interannual variability than at the bog. Overall, the fen functioned as a stronger CO_2 sink, although this pattern was disrupted during the anomalous year 2016. Across all study years, both the fen and the bog acted as sinks of CO_2 during the active-season. The fen was generally a stronger CH_4 source to the atmosphere (Table 1).

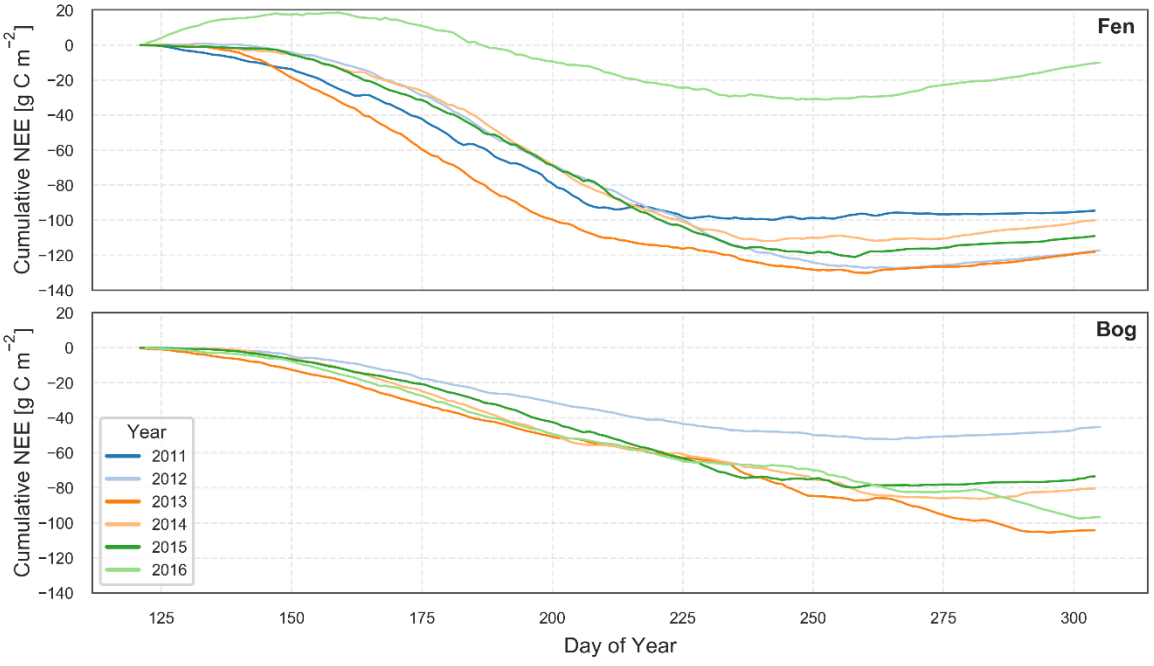

Figure 6: Active-season (May-Oct) cumulative NEE at the Siikaneva fen (top) and bog (bottom) sites for different years. Lines represent gapfilled cumulative sums for individual years plotted against day of year. Years shown in fen are 2011-2016, but for bog 2012-2016.

In 2016, the fen exhibited the highest GPP, TER, and CH_4 cumulative sum, along with the lowest cumulative NEE of all study years. The strongest CO_2 uptake at the fen occurred in 2013 (−118.2 g C m^{-2}) and the smallest in 2016 (−10 g C m^{-2}). The bog had its smallest CO_2 uptake in 2012 (−45.3 g C m^{-2}) and its strongest in 2013 (−104.3 g C m^{-2}).

On average, the fen sequestered 80.8 g C m^{-2}, compared to 72.2 g C m^{-2} at the bog, showing that the fen was on average a stronger carbon sink over the active-season.

The fen generally exhibited greater interannual variability in cumulative NEE during the early active-season, whereas variability in the bog became more pronounced later in the season. This pattern was supported statistically when the anomalous fen year 2016 was excluded (Wilcoxon test, $p < 0.001$).

https://doi.org/10.5194/egusphere-2026-3323
Preprint. Discussion started: 24 June 2026

Table 1: Active-season sums (g C m^{-2}) of GPP, TER, NEE and CH_4 flux for each year and their mean ± standard deviation values over 5 years.

Site	Year	GPP [g C m^{-2}]	TER [g C m^{-2}]	NEE CO_2 [g C m^{-2}]	CH_4 [g C m^{-2}]	NEE + CH_4 [g C m^{-2}]
Fen	2011	-355.6	260.9	-94.7	7.2	-87.4
	2012	-341.8	224.5	-117.3	10.2	-107.2
	2013	-379.8	261.6	-118.2	12.7	-105.5
	2014	-336.7	236.5	-100.1	10.2	-89.9
	2015	-335.2	226.1	-109.1	10.4	-98.7
	2016	-381.6	371.4	-10.2	13.8	3.6
	Mean	**-355.1 ± 21.1**	**263.5 ± 55.3**	**-91.6 ± 41.0**	**10.8 ± 2.3**	**-80.8 ± 42.1**
Bog	2011	NA	NA	NA	NA	NA
	2012	-220.7	175.4	-45.3	7.0	-38.3
	2013	-240.4	136.1	-104.3	9.5	-94.8
	2014	-256.9	176.5	-80.5	9.2	-71.2
	2015	-196.3	122.7	-73.6	7.3	-66.2
	2016	-234.3	137.6	-96.7	6.3	-90.5
	Mean	**-229.8 ± 22.8**	**149.7 ± 24.7**	**-80.1 ± 23.0**	**7.9 ± 1.4**	**-72.2 ± 22.5**

3.3 Drivers

3.3.1 Temperature response

The temperature dependence of daily CH_4 flux across soil depths (5 – 35 cm) indicated that the bog site exhibited relatively stable temperature sensitivity (Q_{10} = 3.38 – 4.44), whereas the fen showed a broader range of responses (Q_{10} = 2.21 – 7.65). Furthermore, at the fen site the temperature dependence of CH_4 flux increased with soil depth (Fig. 7, a-c).

A similar pattern was observed for nighttime NEE. The temperature dependence increased with soil depth at the fen site, whereas no clear depth related pattern was observed at the bog site. In addition, Q_{10} values for nighttime NEE were more stable at the bog (Q_{10} = 3.95 – 4.07) then at the fen (Q_{10} = 3.28 – 5.00) (Fig. 7, d-f).

https://doi.org/10.5194/egusphere-2026-3323
Preprint. Discussion started: 24 June 2026

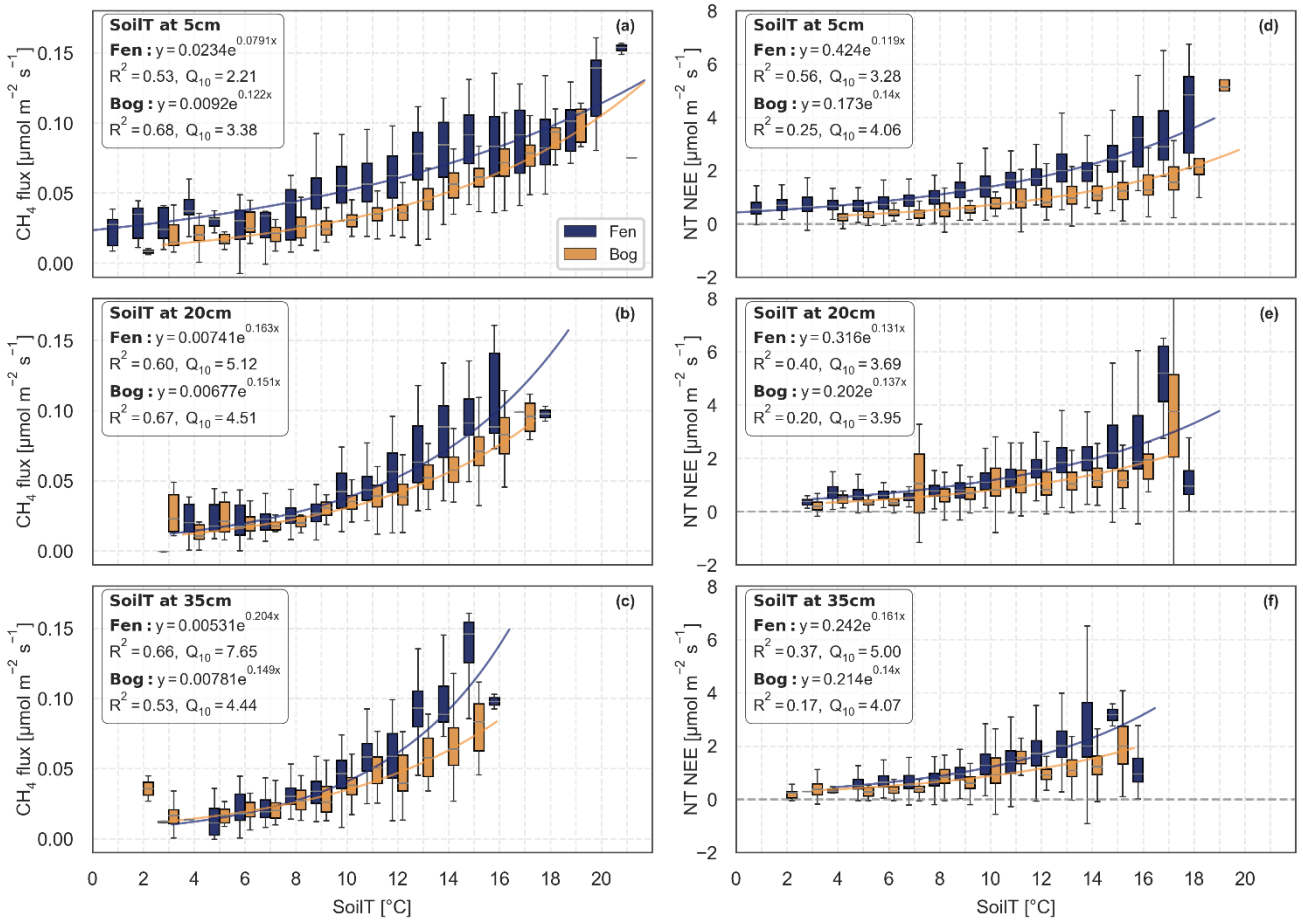

Figure 7: Temperature dependence of daily methane (CH_4) flux as a function of soil temperature at depths of 5 (a), 20 (b) and 35 cm (c) and 30-min nighttime (NT) net ecosystem exchange (NEE) on soil temperature at depths of 5 (d), 20 (e) and 35 cm (f) at the fen (blue) and bog (orange) sites during the active-season (May–Oct). Nighttime NEE was defined as CO_2 flux observations measured under low-light conditions (PAR < 10 µmol m^{-2} s^{-1}). Boxplots show the distribution of fluxes within 1 °C soil temperature bins; boxes represent the interquartile range, the horizontal line indicates the median, and whiskers extend to 1.5 times the interquartile range. Exponential models were fitted to flux observations for each site (lines).

3.3.2 Vegetation structure

CH_4 fluxes had positive linear relationships with both LAI_{Tot} (Fig. 8a) and LAI_{Aer} (Fig. 8b) in both ecosystems ($p < 0.0001$). Similarly, GPP increased with both LAI_{Tot} (Fig. 8c) and LAI_{Aer} (Fig. 8d) across both ecosystems ($p < 0.001$). Linear mixed-effects models confirmed significant positive LAI effects on CH_4 fluxes, whereas LAI × ecosystem interactions were not significant ($p = 0.15$–0.91), indicating similar response slopes between the fen and bog ecosystems.

However, models including LAI_{Aer} explained CH_4 variability better than models based on LAI_{Tot} alone. Partial correlation analysis further demonstrated that the relationship between CH_4 flux and LAI_{Tot} disappeared after accounting for LAI_{Aer},

https://doi.org/10.5194/egusphere-2026-3323
Preprint. Discussion started: 24 June 2026

whereas LAI_{Aer} remained significantly correlated with CH_4 flux after accounting for LAI_{Tot}, indicating that aerenchymatous vegetation rather than total vegetation density primarily explained CH_4 variability.

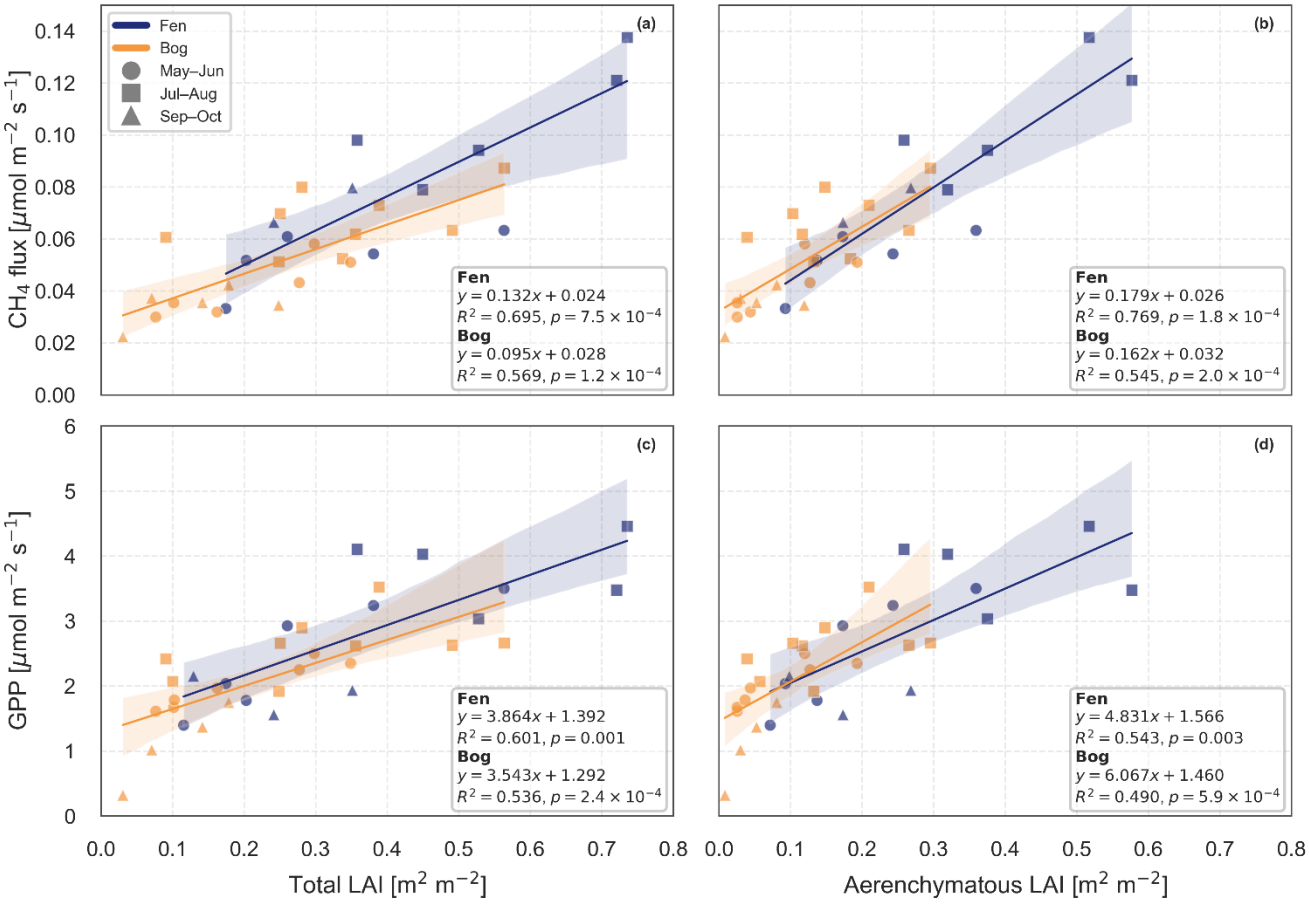

Figure 8: Top panels: CH_4 flux as a function of total LAI (a) and aerenchymatous LAI (b). Bottom panels: GPP as a function of total LAI (c) and aerenchymatous LAI (d). Points represent monthly mean values, and different marker shapes indicate May-Jun, Jul-Aug and Sept-Oct. Years shown from bog are 2012–2016 (orange) and from fen 2014–2016 (blue). Solid lines and shaded areas represent site-specific linear regressions and their 95% confidence intervals, respectively.

3.3.3 Seasonal variation of CH_4 exchange

CH_4 fluxes increased exponentially with both soil temperature and GPP in the fen and bog sites (Fig. 7 & Fig. 9). However, the relationships differed between the two periods (May–Jul & Aug–Oct) within the active-season. Consistent with the broader seasonal spread of the fen centroids in the PCA (Fig. 5), this was particularly apparent in the fen where CH_4 fluxes were consistently higher during the late active-season at a given soil temperature or GPP, resulting in a clear seasonal hysteresis pattern. In contrast, the bog exhibited a weaker seasonal separation and a more consistent response throughout the season. Seasonal divergence between early- and late-season relationships was apparent for GPP, although the separation was more pronounced in the fen.

https://doi.org/10.5194/egusphere-2026-3323
Preprint. Discussion started: 24 June 2026

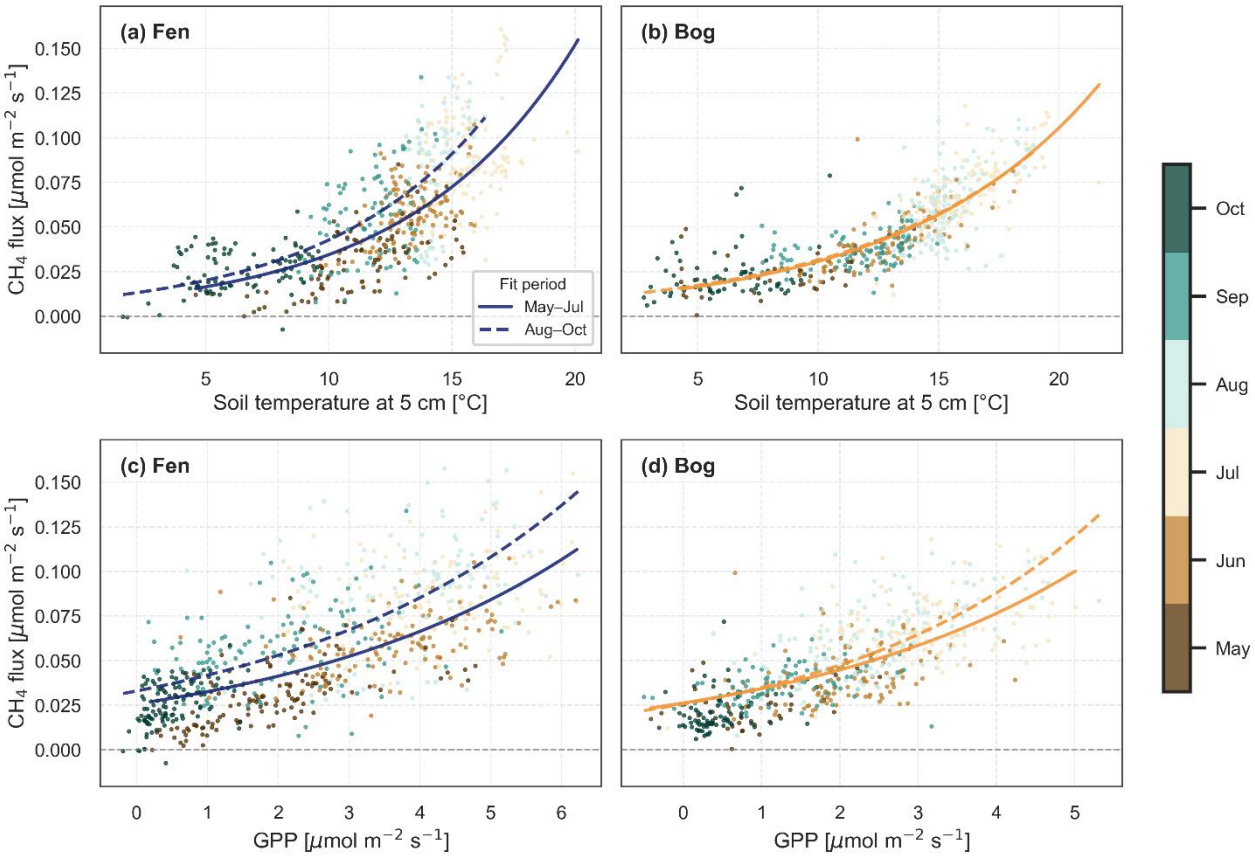

Figure 9: Relationship between daily mean CH_4 flux and soil temperature at 5 cm depth in the fen (a) and bog (b), and between daily mean CH_4 flux and GPP in the fen (c) and bog (d) during the active-season (May–Oct). Points are coloured by month. Lines show exponential fits fitted separately for the early season (May–Jul; solid line) and late season (Aug–Oct; dashed line). Stronger separation between early- and late-season fits indicates a more pronounced seasonal hysteresis in both the temperature and GPP response of CH_4 flux.

Monthly mean CH_4 flux and GPP exhibited hysteretic seasonal trajectories at both sites (Fig. 10a), with CH_4 fluxes lagging behind changes in GPP during the seasonal cycle. The hysteresis patterns were more pronounced in the fen, which showed larger seasonal excursions and higher CH_4 fluxes than the bog. Lag-correlation analysis further demonstrated delayed coupling between GPP and CH_4 emissions (Fig. 10b), with maximum correlations occurring at lag times of 11 days in the fen and 7 days in the bog.

https://doi.org/10.5194/egusphere-2026-3323
Preprint. Discussion started: 24 June 2026

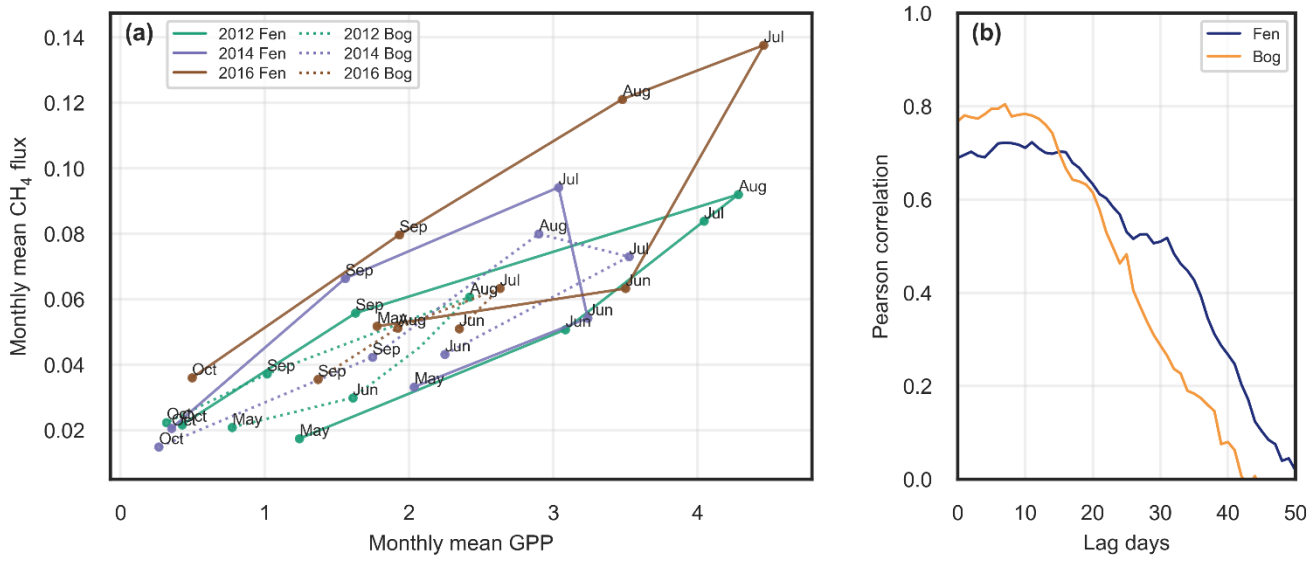

Figure 10: (a) Relationship between monthly mean CH_4 flux and monthly mean GPP for the fen and bog sites. Lines connect monthly means within each year, with solid lines representing the fen and dotted lines representing the bog; colours indicate individual years. Month labels indicate the seasonal progression. (b) Pearson correlations between daily CH_4 flux and GPP across lag times from 0 to 50 days for each site.

3.3.4 Seasonal variation of photosynthetic parameters

Seasonal variation in CO_2 exchange differed between ecosystems, with the fen exhibiting stronger seasonal shifts in GPP and NEE than the bog, consistent with the broader separation of fen centroids along the corresponding flux vectors in the PCA (Fig. 5). Daily GPP, TER and NEE all peaked during the mid-season at both sites, but seasonal amplitudes were larger at the fen, with greater centroid separation and broader within-season ellipses for the fen indicated stronger seasonal variability in CO_2 exchange compared with the bog (Fig. 5).

To further examine seasonal differences in photosynthetic functioning we fitted light-response curves that indicated higher modelled maximum GPP at the fen than at the bog (Fig. 11a). The seasonal peak in P_{max} occurred earlier in the sedge-dominated fen, where maximum values were typically observed during July, whereas P_{max} at the moss- and shrub-dominated bog generally peaked later, during August (Fig. 11b). Across years, peak P_{max} at the fen occurred either earlier than or concurrently with the bog, but never later. Mean active-season P_{max} was 55.1% higher at the fen than at the bog, while peak P_{max} values at the fen exceeded those at the bog by 54.6%. The fen also exhibited consistently greater seasonal amplitudes and steeper rates of seasonal increase in P_{max}, indicating more rapid early enhancement of photosynthetic capacity compared to the bog. Rates of seasonal P_{max} increase were consistently greater at the fen across all years. The fen also exhibited higher LUE throughout the active-season, although LUE reached maximum values in July at both sites (Fig. 11c). Mean active-season LUE exceeded bog values by 77.6%, while peak LUE values at the fen were 102.7% higher than those observed at the bog.

https://doi.org/10.5194/egusphere-2026-3323
Preprint. Discussion started: 24 June 2026

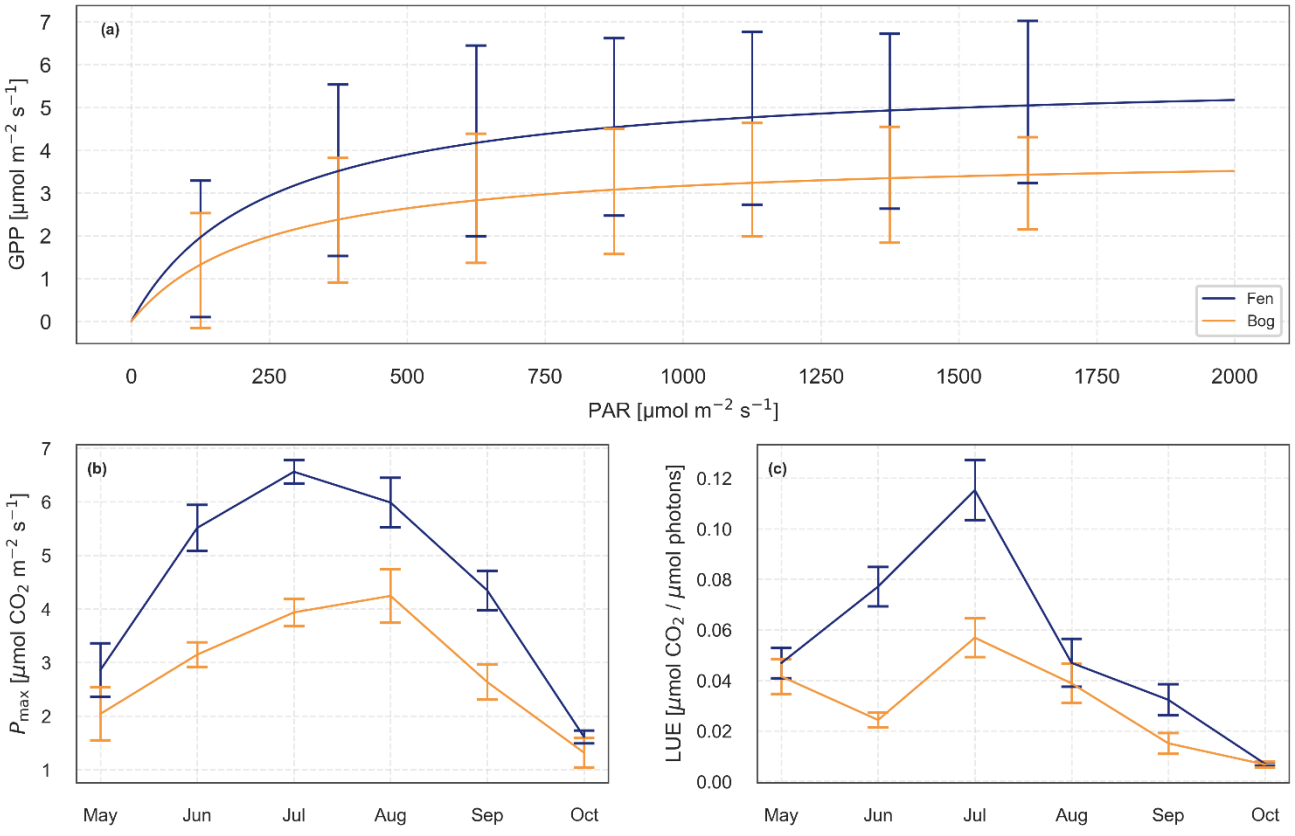

Figure 11: (a) Light response curves of gross primary production (GPP) as a function of photosynthetically active radiation (PAR). Solid lines show fitted light response curves estimated using nonlinear least squares with air temperature fixed at the mean observed value for each site. Error bars represent ±1 standard deviation of GPP within 250 µmol m^{-2} s^{-1} PAR bins. Only non-zero GPP values and PAR > 10 µmol m^{-2} s^{-1} were included. (b) Seasonal variation in maximum photosynthetic capacity (P_{max}), defined as the modelled maximum GPP derived from the fitted light response curves evaluated across the full PAR range (0–2000 µmol m^{-2} s^{-1}). Monthly P_{max} values were estimated for each year, month and ecosystem and averaged across years; error bars denote ±1 standard error. (c) Seasonal variation in light-use efficiency (LUE), calculated as the ratio of daily GPP to PAR, excluding PAR < 10 µmol m^{-2} s^{-1}. Values were averaged by month across all study years (2011–2016); points represent monthly means and error bars ±1 standard error.

Interannual variability in P_{max} differed between ecosystems and across the active-season. The highest variability occurred in May at the fen (SD = 1.23) and in August at the bog (SD = 1.00). Overall seasonal variability in P_{max} was greater at the fen than at the bog (mean SD = 0.79 and 0.68, respectively). Relative variability in P_{max} was highest in May at both sites and lowest in July, while the bog exhibited higher relative variability than the fen from July onwards, particularly during October.

Linear mixed-effects modelling revealed significant seasonal variation in P_{max}, with higher values during June–August relative to May. Significant ecosystem × month interactions during June and July indicated differing seasonal trajectories between ecosystems. Seasonal trajectories of P_{max} diverged most strongly during June and July, whereas ecosystem differences weakened later in the active-season.

https://doi.org/10.5194/egusphere-2026-3323
Preprint. Discussion started: 24 June 2026

In contrast to P_{max}, seasonal trajectories of LUE did not differ significantly between ecosystems. Linear mixed-effects modelling revealed significant effects of both ecosystem type and month on LUE, whereas the ecosystem × month interaction was not significant. This indicates that although LUE remained consistently higher at the fen throughout the active-season, the temporal pattern of seasonal development was broadly similar between ecosystems.

4 Discussion

4.1 Vegetation structure and productivity drive stronger CO_2 uptake in the fen

Our results demonstrate significant differences in carbon dynamics between the fen and bog sites despite shared climate conditions. In contrast to our hypothesis (i) and several previous studies (e.g. Saarnio et al., 2009; Turetsky et al., 2014; Turunen et al., 2002), the fen acted as a stronger CO_2 sink than the bog during the active-season. This difference was accompanied by consistently higher total and aerenchymatous LAI at the fen, indicating that vegetation structure and phenology were important controls on the ecosystem scale carbon assimilation. Given the shared climate at the sites, these observed differences are most plausibly explained by ecosystem characteristics such as vegetation composition, productivity and microtopography, rather than climate.

The fitted light response curves further supported this interpretation, indicating higher modelled maximum GPP at the fen than the bog (Fig. 11a). In addition, the fen exhibited higher LUE (Fig. 11b), suggesting more efficient use of incoming radiation for carbon assimilation. Together, these results indicate that the greater abundance of photosynthetically active vegetation at the fen contributed to its higher CO_2 uptake. Although WTD fluctuated more at the fen, the ecosystem maintained higher GPP and remained a stronger CO_2 sink during the active-season, suggesting that higher productivity buffered the effects of occasional water table drawdown.

Previous comparisons of adjacent fens and bogs have reported contrasting patterns of CO_2 exchange compared with our findings. For example, Humphreys et al. (2006) reported similar summer NEE between adjacent poor fen and bog sites in Ottawa. A key difference is that LAI was higher at the bog than at the fen in that study, whereas the Siikaneva fen consistently exhibited higher LAI. This contrast in vegetation structure may partly explain why active-season CO_2 uptake was greater at the fen in our study. Furthermore, the Ottawa bog was shrub dominated, likely supporting greater photosynthetic biomass than the Siikaneva bog. In addition, the Ottawa study was based on a single summer, the longer observational period in our study captured substantial interannual variability, which may not be resolved in shorter datasets. These findings suggest that assumptions of fens as universally weaker CO_2 sinks than bogs may lead to underestimation of their carbon sequestration potential under certain conditions.

https://doi.org/10.5194/egusphere-2026-3323
Preprint. Discussion started: 24 June 2026

4.2 Vegetation drives stronger CH_4 emissions in the fen

Consistent with our hypothesis (ii), the fen emitted substantially more CH_4 than the bog, likely reflecting a combination of higher primary productivity providing labile carbon substrates for methanogenesis and greater abundance of aerenchymatous vegetation facilitating plant-mediated CH_4 transport (Jentzsch et al., 2024; Korrensalo et al., 2022).

Soil temperature was strongly correlated between the two ecosystems. Because temperature conditions were similar, differences in CH_4 flux dynamics between the sites are unlikely to be explained by temperature alone. Instead, differences in vegetation abundance, species composition, and microtopography likely contributed substantially to the contrasting CH_4 flux dynamics observed at the fen and bog, supporting the mechanism underlying hypothesis (ii).

The stronger seasonal development of vascular vegetation in the fen may explain the more pronounced hysteresis observed between CH_4 emissions and GPP compared to the bog (Fig. 10a). Similar hysteretic relationships have previously been reported across peatlands, where CH_4 emissions respond to seasonal changes in productivity (Chang et al., 2020; Rinne et al., 2018) and temperature (Chang et al., 2021, 2020) with a temporal lag. This lag is commonly attributed to microbial substrate-mediated CH_4 production hysteresis, whereby CH_4 production depends not only on concurrent environmental conditions, but also on the seasonal accumulation and delayed microbial processing of recently assimilated carbon substrates (Chang et al., 2020). As photosynthetic activity increases during the active-season, plant-derived carbon is transferred belowground and can stimulate methanogenesis after a delay, resulting in seasonal offsets between peak productivity and peak CH_4 emissions.

The more pronounced hysteresis observed in the fen may reflect stronger seasonal development of vascular vegetation, which likely increased the supply of recently assimilated carbon and stimulated methanogenesis through greater substrate availability. This interpretation is consistent with Chang et al. (2020), who linked seasonal CH_4 hysteresis to delayed microbial processing of plant-derived substrates and temporal lags between photosynthesis and methane production.

4.3 CO_2 and CH_4 fluxes of the fen exhibit stronger temporal dynamics than the bog

Consistent with hypothesis (iii), the fen exhibited greater temporal variability in both CO_2 and CH_4 fluxes compared to the bog (Fig. 3), also supporting previous findings that bogs tend to have more stable temporal variability than fens (Leppälä et al., 2009). Seasonal NEE varied more strongly at the fen, and CH_4 emissions spanned a wider range. Moreover, a more pronounced hysteresis behaviour between CH_4 flux and GPP was observed in the fen than the bog (Fig. 10a). In addition, temperature sensitivities (Q_{10}) for both CH_4 and nighttime NEE showed greater variability across soil depths in the fen when compared with the bog (Fig. 7). This suggests that temperature control of both methanogenesis and ecosystem respiration becomes stronger with depth at the fen peat profile, indicating stronger coupling between deep peat processes and temperature in the fen, whereas temperature sensitivity remains more uniform across depths in the bog.

Together, these patterns indicate that carbon exchange at the fen is more responsive to environmental variability, while the bog is comparatively buffered. This supports the view of bogs as more stable systems dominated by *Sphagnum* and evergreen shrubs, while fens, driven by vascular plant productivity, exhibit stronger temporal dynamics. These patterns are consistent

https://doi.org/10.5194/egusphere-2026-3323
Preprint. Discussion started: 24 June 2026

with the multivariate relationships revealed by the PCA (Fig. 5), which integrates fluxes and environmental variables across sites and seasons. The ordination showed a clearer separation of fen site–season centroids compared to the bog, as well as larger within-season variability in the fen. In addition, vectors for GPP and CH_4 were oriented towards the fen centroids, confirming that higher productivity and methane emissions characterise this ecosystem. In contrast, bog centroids were more tightly clustered, indicating more constrained flux dynamics across seasonal phases.

Seasonal flux dynamics differed between the ecosystems. The bog showed weaker seasonal variability in both CO_2 and CH_4 fluxes than the fen. This difference likely reflects contrasting vegetation structure. The bog vegetation is dominated by evergreen shrubs and Sphagnum mosses while the fen is dominated by sedges that develop new aboveground biomass each year. These phenological differences provide a consistent explanation for the stronger seasonal variability observed in C fluxes at the fen, consistent with hypothesis (iii).

The stronger diurnal amplitude in CO_2 exchange at the fen further supports hypothesis (iii). This pattern likely reflects the higher productivity and greater LAI at the fen. Higher photosynthetic uptake during daytime increases the availability of recently assimilated carbon, which can subsequently enhance ecosystem respiration during nighttime periods.

CH_4 fluxes showed weak or less consistent diurnal variability than CO_2 fluxes. Previous studies at the Siikaneva fen have similarly reported an absence of a consistent diurnal cycle when examined over longer periods, such as July–September (Rinne et al., 2007) or the full annual record (Rinne et al., 2018). However, when the data were analysed month by month, some diurnal variability became apparent, particularly in May and July. This variability may partly reflect plant-mediated methane transport, as the abundance of aerenchymatous plants can facilitate CH_4 transport from peat to the atmosphere and contribute to short term variability in emissions (van den Berg et al., 2016). On the other hand, measurement related effects related to air density correction (Webb et al., 1980; Jentzsch et al., 2021) may also contribute to apparent diurnal patterns, especially for the bog site where an open path CH_4 analyser was used. These effects should therefore be considered when interpreting short term CH_4 flux variability.

Vegetation phenology differed between the ecosystems, as peak P_{max} occurred earlier in the sedge-dominated fen (July) than in the moss- and shrub-dominated bog (August, Fig. 11c). Consistent with this pattern, the fen exhibited more interannual variability in NEE during the early active-season, whereas the bog showed greater variability later in the season (Fig. 6). This likely reflects earlier seasonal development of vascular plant productivity in the fen, in agreement with the findings of Leppälä et al. (2009), who showed that sedges tend to peak earlier in the active-season than shrubs and mosses.

Interannual variability was particularly evident in 2016, which stood out as an anomalous year at the fen. During that year, the fen exhibited the weakest net CO_2 uptake and the highest cumulative CH_4 emissions of the study period. Notably, it was also the only year in which the fen acted as a weaker CO_2 sink than the bog, consistent with hypothesis (i). Previous work has attributed anomalously high spring CO_2 emissions in 2016 to warm deep soil temperatures combined with frozen surface layers restricting gas diffusion during the previous winter months (Särkelä et al., 2025).

Previous work within the Siikaneva peatland complex has shown strong spatial variation in carbon fluxes across plant communities and surface types associated with hydrological gradients (Korrensalo et al., 2020; Männistö et al., 2019; Riutta

https://doi.org/10.5194/egusphere-2026-3323
Preprint. Discussion started: 24 June 2026

et al., 2007), whereas temporal variability at the ecosystem scale is less strongly explained by water table depth alone (Rinne et al., 2018). These spatial differences arise because microtopography and vegetation structure create persistent differences in WTD between microsites. This interpretation is further supported by the PCA (Fig 6.), where GPP aligned closely with PAR, indicating a strong light limitation of photosynthesis, while CH_4 showed a weaker but consistent association with WTD. The shorter vector length of WTD suggests that, although hydrology influences fluxes, it explains less of the overall variability than radiation and productivity-related factors.

4.4 Implications of ongoing fen-to-bog transition for carbon cycling

Recent evidence from the Siikaneva wetland complex suggests that ongoing ombrotrophication is already shifting parts of the fen system toward more bog-like vegetation (Korrensalo et al., 2025). In the context of fen-to-bog transition, our findings suggest that shifts toward bog-like vegetation and structure may reduce CH_4 emissions and dampen temporal variability in carbon fluxes, consistent with previous understanding of peatland succession. However, the effect on CO_2 uptake appears less predictable. While bogs are often assumed to function as stronger CO_2 sinks, our results show that fens can exceed bogs in carbon uptake under certain conditions, particularly where vascular plant productivity is high. This highlights the need for caution when generalising peatland carbon dynamics across ecosystem types and suggests that vegetation composition and phenology play a more important role in regulating carbon exchange than peatland classification alone.

5 Conclusion

Overall, our results demonstrate that fens can, under certain conditions, act simultaneously as stronger CO_2 sinks and stronger CH_4 sources than adjacent bogs. In the Siikaneva wetland complex, the fen exhibited greater photosynthetic capacity, higher LAI and LUE than the bog, resulting in stronger active-season CO_2 uptake, despite greater variability in hydrological conditions. At the same time, the fen emitted substantially more CH_4 than the bog, likely reflecting both greater primary productivity and the higher abundance of aerenchymatous plants that facilitate CH_4 transport.

These findings highlight the importance of vegetation structure and phenology in regulating peatland carbon exchange. Models that assume fixed carbon flux patterns based solely on peatland type may therefore underestimate the role of vegetation composition in determining ecosystem carbon balance. In the context of fen-bog transitions, shifts towards bog like vegetation may reduce CH_4 emissions, but do not necessarily imply stronger CO_2 sequestration. Incorporating vegetation dynamics into peatland carbon models will therefore be essential for improving predictions of peatland climate feedbacks under future environmental change.

https://doi.org/10.5194/egusphere-2026-3323
Preprint. Discussion started: 24 June 2026

Appendix A

Table A1: Data availability from May-Oct of CO_2 and CH_4 flux in the fen and bog

Year	CO_2 Fen	CH_4 Fen	CO_2 Bog	CH_4 Bog
2011	43.4%	37.5%	25.8%	14.7%
2012	61.2%	60.3%	51.1%	35.6%
2013	61.2%	61.6%	13.0%	35.9%
2014	28.1%	28.3%	47.8%	39.1%
2015	45.3%	12.2%	44.2%	38.9%
2016	48.9%	39.6%	40.1%	23.3%

Data availability

Data used for the analyses are available at https://smear.avaa.csc.fi/

Author contributions

TV, E-ST. and IM conceived and designed the study. EGG carried out data analysis and wrote the main manuscript. EM and AK created and structured the PCA analysis. All authors have contributed to the research and revisions of the manuscript.

Competing interests

The authors declare no competing interests.

Acknowledgements

We thank the Hyytiälä Forestry Field Station for providing research facilities and the technical staff for their continuous support in maintaining the measurement systems and ensuring smooth instrument operation. We also thank Pasi Kolari for assistance with data gapfilling and flux partitioning.

We acknowledge the use of Grammarly (https://www.grammarly.com/, last access: 27 May 2026) for grammar checking and improving text clarity during manuscript preparation. We further acknowledge the use of ChatGPT (https://chatgpt.com/, last access: 27 May 2026) for language refinement and assistance with code improvement during manuscript preparation. All scientific interpretations, analyses, and conclusions were developed and verified by the authors.

https://doi.org/10.5194/egusphere-2026-3323
Preprint. Discussion started: 24 June 2026

Financial support

This study has received financial support from the Research Council of Finland project N-PERM (Grant No. 341348) and projects 338980, 360071 and 371011.

EU Horizon Europe-Framework Programme for Research and Innovation (Grant No. 101056921-GreenFeedBack and LiweFor No. 101079192) and ICOS-FI via funding from the University of Helsinki.

References

Abdalla, M., Hastings, A., Truu, J., Espenberg, M., Mander, Ü., and Smith, P.: Emissions of methane from northern peatlands: a review of management impacts and implications for future management options, Ecol Evol, 6, 7080–7102, https://doi.org/10.1002/ece3.2469, 2016.

Alekseychik, P., Korrensalo, A., Mammarella, I., Launiainen, S., Tuittila, E.-S., Korpela, I., and Vesala, T.: Carbon balance of a Finnish bog: temporal variability and limiting factors based on 6 years of eddy-covariance data, Biogeosciences, 18, 4681–4704, https://doi.org/10.5194/bg-18-4681-2021, 2021.

Aubinet, M., Vesala, T., and Papale, D. (Eds.): Eddy covariance: a practical guide to measurement and data analysis, Springer, Dordrecht ; New York, 438 pp., 2012.

van den Berg, M., Ingwersen, J., Lamers, M., and Streck, T.: The role of *Phragmites* in the CH_4 and CO_2 fluxes in a minerotrophic peatland in southwest Germany, Biogeosciences, 13, 6107–6119, https://doi.org/10.5194/bg-13-6107-2016, 2016.

van den Berg, M., van den Elzen, E., Ingwersen, J., Kosten, S., Lamers, L. P. M., and Streck, T.: Contribution of plant-induced pressurized flow to CH4 emission from a Phragmites fen, Sci Rep, 10, 12304, https://doi.org/10.1038/s41598-020-69034-7, 2020.

Blodau, C., Basiliko, N., and Moore, T. R.: Carbon turnover in peatland mesocosms exposed to different water table levels, Biogeochemistry, 67, 331–351, https://doi.org/10.1023/B:BIOG.0000015788.30164.e2, 2004.

Bond-Lamberty, B. and Thomson, A.: Temperature-associated increases in the global soil respiration record, Nature, 464, 579–582, https://doi.org/10.1038/nature08930, 2010.

Bubier, J. L., Crill, P. M., Moore, T. R., Savage, K., and Varner, R. K.: Seasonal patterns and controls on net ecosystem CO2 exchange in a boreal peatland complex, Global Biogeochemical Cycles, 12, 703–714, https://doi.org/10.1029/98GB02426, 1998.

Chang, K.-Y., Riley, W. J., Crill, P. M., Grant, R. F., and Saleska, S. R.: Hysteretic temperature sensitivity of wetland CH_4 fluxes explained by substrate availability and microbial activity, Biogeosciences, 17, 5849–5860, https://doi.org/10.5194/bg-17-5849-2020, 2020.

Chang, K.-Y., Riley, W. J., Knox, S. H., Jackson, R. B., McNicol, G., Poulter, B., Aurela, M., Baldocchi, D., Bansal, S., Bohrer, G., Campbell, D. I., Cescatti, A., Chu, H., Delwiche, K. B., Desai, A. R., Euskirchen, E., Friborg, T., Goeckede, M., Helbig, M., Hemes, K. S., Hirano, T., Iwata, H., Kang, M., Keenan, T., Krauss, K. W., Lohila, A., Mammarella, I., Mitra, B., Miyata, A., Nilsson, M. B., Noormets, A., Oechel, W. C., Papale, D., Peichl, M., Reba, M. L., Rinne, J., Runkle, B. R. K., Ryu, Y., Sachs, T., Schäfer, K. V. R., Schmid, H. P., Shurpali, N., Sonnentag, O., Tang, A. C. I., Torn, M. S., Trotta, C.,

https://doi.org/10.5194/egusphere-2026-3323
Preprint. Discussion started: 24 June 2026

Tuittila, E.-S., Ueyama, M., Vargas, R., Vesala, T., Windham-Myers, L., Zhang, Z., and Zona, D.: Substantial hysteresis in emergent temperature sensitivity of global wetland CH4 emissions, Nat Commun, 12, 2266, https://doi.org/10.1038/s41467-021-22452-1, 2021.

Charman, D. J.: Peatlands and environmental change, J. Wiley, Chichester, West Sussex, England ; New York, 301 pp., 2002.

Chen, S., Zhang, M., Zou, J., and Hu, Z.: Relationship between basal soil respiration and the temperature sensitivity of soil respiration and their key controlling factors across terrestrial ecosystems, J Soils Sediments, 22, 769–781, https://doi.org/10.1007/s11368-021-03130-7, 2022.

Drebs, A. (Ed.): Tilastoja Suomen ilmastosta 1971-2000 =: Climatological statistics of Finland 1971-2000, Ilmatieteen laitos, Helsinki, 99 pp., 2002.

Evans, D. E.: Aerenchyma formation, New Phytologist, 161, 35–49, https://doi.org/10.1046/j.1469-8137.2003.00907.x, 2004.

Gorham, E.: Northern Peatlands: Role in the Carbon Cycle and Probable Responses to Climatic Warming, Ecological Applications, 1, 182–195, https://doi.org/10.2307/1941811, 1991.

Humphreys, E. R., Lafleur, P. M., Flanagan, L. B., Hedstrom, N., Syed, K. H., Glenn, A. J., and Granger, R.: Summer carbon dioxide and water vapor fluxes across a range of northern peatlands, Journal of Geophysical Research: Biogeosciences, 111, https://doi.org/10.1029/2005JG000111, 2006.

Järvi-Laturi, E., Tahvanainen, T., Koskinen, E., López-Blanco, E., Lämsä, J., Marttila, H., Mastepanov, M., Paavola, R., Väisänen, M., and Christensen, T. R.: Plant community composition explains spatial variation in year-round methane fluxes in a boreal rich fen, Biogeosciences, 22, 6343–6367, https://doi.org/10.5194/bg-22-6343-2025, 2025.

Jentzsch, K., Boike, J., and Foken, T.: Importance of the Webb, Pearman, and Leuning (WPL) correction for the measurement of small CO_2 fluxes, Atmospheric Measurement Techniques, 14, 7291–7296, https://doi.org/10.5194/amt-14-7291-2021, 2021.

Jentzsch, K., Männistö, E., Marushchak, M. E., Korrensalo, A., van Delden, L., Tuittila, E.-S., Knoblauch, C., and Treat, C. C.: Shoulder season controls on methane emissions from a boreal peatland, Biogeosciences, 21, 3761–3788, https://doi.org/10.5194/bg-21-3761-2024, 2024.

Juottonen, H., Galand, P. E., Tuittila, E.-S., Laine, J., Fritze, H., and Yrjälä, K.: Methanogen communities and Bacteria along an ecohydrological gradient in a northern raised bog complex, Environmental Microbiology, 7, 1547–1557, https://doi.org/10.1111/j.1462-2920.2005.00838.x, 2005.

Kettunen, A., Kaitala, V., Alm, J., Silvola, J., Nykänen, H., and Martikainen, P.: Predicting variations in methane emissions from boreal peatlands through regression models, Boreal Environment Research, 5, 115–131, 2000.

Kim, JooN., Verma, S. B., and Billesbach, D. P.: Seasonal variation in methane emission from a temperate Phragmites-dominated marsh: effect of growth stage and plant-mediated transport, Global Change Biology, 5, 433–440, https://doi.org/10.1046/j.1365-2486.1999.00237.x, 1999.

Koelbener, A., Ström, L., Edwards, P. J., and Olde Venterink, H.: Plant species from mesotrophic wetlands cause relatively high methane emissions from peat soil, Plant Soil, 326, 147–158, https://doi.org/10.1007/s11104-009-9989-x, 2010.

Kolari, T. H. M. and Tahvanainen, T.: Inference of future bog succession trajectory from spatial chronosequence of changing aapa mires, Ecology and Evolution, 13, e9988, https://doi.org/10.1002/ece3.9988, 2023.

https://doi.org/10.5194/egusphere-2026-3323
Preprint. Discussion started: 24 June 2026

Kolari, T. H. M., Sallinen, A., Wolff, F., Kumpula, T., Tolonen, K., and Tahvanainen, T.: Ongoing Fen–Bog Transition in a Boreal Aapa Mire Inferred from Repeated Field Sampling, Aerial Images, and Landsat Data, Ecosystems, 25, 1166–1188, https://doi.org/10.1007/s10021-021-00708-7, 2022.

Korpela, I., Haapanen, R., Korrensalo, A., Tuittila, E.-S., and Vesala, T.: Fine-resolution Mapping of Microforms of a Boreal Bog Using Aerial Images and Waveform-Recording LiDAR, mires-and-peat, 26, https://doi.org/10.19189/MaP.2018.OMB.388, 2020.

Korrensalo, A., Hájek, T., Vesala, T., Mehtätalo, L., and Tuittila, E.-S.: Variation in photosynthetic properties among bog plants, Botany, 94, 1127–1139, https://doi.org/10.1139/cjb-2016-0117, 2016.

Korrensalo, A., Alekseychik, P., Hájek, T., Rinne, J., Vesala, T., Mehtätalo, L., Mammarella, I., and Tuittila, E.-S.: Species-specific temporal variation in photosynthesis as a moderator of peatland carbon sequestration, Biogeosciences, 14, 257–269, https://doi.org/10.5194/bg-14-257-2017, 2017.

Korrensalo, A., Kettunen, L., Laiho, R., Alekseychik, P., Vesala, T., Mammarella, I., and Tuittila, E.-S.: Boreal bog plant communities along a water table gradient differ in their standing biomass but not their biomass production, Journal of Vegetation Science, 29, 136–146, https://doi.org/10.1111/jvs.12602, 2018.

Korrensalo, A., Mehtätalo, L., Alekseychik, P., Uljas, S., Mammarella, I., Vesala, T., and Tuittila, E.-S.: Varying Vegetation Composition, Respiration and Photosynthesis Decrease Temporal Variability of the CO2 Sink in a Boreal Bog, Ecosystems, 23, 842–858, https://doi.org/10.1007/s10021-019-00434-1, 2020.

Korrensalo, A., Mammarella, I., Alekseychik, P., Vesala, T., and Tuittila, E.-S.: Plant mediated methane efflux from a boreal peatland complex, Plant Soil, 471, 375–392, https://doi.org/10.1007/s11104-021-05180-9, 2022.

Korrensalo, A., Kettunen, J., Mehtätalo, L., Vanhatalo, J., and Tuittila, E.-S.: Detecting Subtle Change in Species and Trait Composition and Quantifying Its Uncertainty in a Boreal Peatland, Journal of Vegetation Science, 36, e70025, https://doi.org/10.1111/jvs.70025, 2025.

Kübert, A., Lohila, A., Vekuri, H., Hatakka, J., Laurila, T., Mäkelä, T., Rainne, J., Suopajärvi, S., Tuovinen, J.-P., and Aurela, M.: Summer temperatures largely control annual methane budgets of a northern Peatland, Agricultural and Forest Meteorology, 381, 111101, https://doi.org/10.1016/j.agrformet.2026.111101, 2026.

Kusin, K., Ogawa, K., Doi, H., Tokida, T., Hirano, T., Jaya, A., and Itoh, M.: Increasing the pH of tropical peat can enhance methane production and methanogenic growth under anoxic conditions, CATENA, 250, 108791, https://doi.org/10.1016/j.catena.2025.108791, 2025.

Laine, A. M., Bubier, J., Riutta, T., Nilsson, M. B., Moore, T. R., Vasander, H., and Tuittila, E.-S.: Abundance and composition of plant biomass as potential controls for mire net ecosytem CO2 exchange, Botany, 90, 63–74, https://doi.org/10.1139/b11-068, 2012.

Leppälä, M., Kukko-Oja, K., Laine, J., and Tuittila, E.-S.: Seasonal dynamics of CO2 exchange during primary succession of boreal mires as controlled by phenology of plants, Ecoscience, 15, 460–471, https://doi.org/10.2980/15-4-3142, 2009.

Leppälä, M., Oksanen, J., and Tuittila, E.-S.: Methane flux dynamics during mire succession, Oecologia, 165, 489–499, https://doi.org/10.1007/s00442-010-1754-6, 2011.

https://doi.org/10.5194/egusphere-2026-3323
Preprint. Discussion started: 24 June 2026

Limpens, J., Berendse, F., Blodau, C., Canadell, J. G., Freeman, C., Holden, J., Roulet, N., Rydin, H., and Schaepman-Strub, G.: Peatlands and the carbon cycle: from local processes to global implications – a synthesis, Biogeosciences, 5, 1475–1491, https://doi.org/10.5194/bg-5-1475-2008, 2008.

Loisel, J. and Yu, Z.: Recent acceleration of carbon accumulation in a boreal peatland, south central Alaska, Journal of Geophysical Research: Biogeosciences, 118, 41–53, https://doi.org/10.1029/2012JG001978, 2013.

Mammarella, I., Peltola, O., Nordbo, A., Järvi, L., and Rannik, Ü.: Quantifying the uncertainty of eddy covariance fluxes due to the use of different software packages and combinations of processing steps in two contrasting ecosystems, Atmospheric Measurement Techniques, 9, 4915–4933, https://doi.org/10.5194/amt-9-4915-2016, 2016.

Männistö, E., Korrensalo, A., Alekseychik, P., Mammarella, I., Peltola, O., Vesala, T., and Tuittila, E.-S.: Multi-year methane ebullition measurements from water and bare peat surfaces of a patterned boreal bog, Biogeosciences, 16, 2409–2421, https://doi.org/10.5194/bg-16-2409-2019, 2019.

Männistö, E., Ylänne, H., Losoi, M., Keinänen, M., Yli-Pirilä, P., Korrensalo, A., Bäck, J., Hellén, H., Virtanen, A., and Tuittila, E.-S.: Emissions of biogenic volatile organic compounds from adjacent boreal fen and bog as impacted by vegetation composition, Science of The Total Environment, 858, 159809, https://doi.org/10.1016/j.scitotenv.2022.159809, 2023.

Mathijssen, P. J. H., Väliranta, M., Korrensalo, A., Alekseychik, P., Vesala, T., Rinne, J., and Tuittila, E.-S.: Reconstruction of Holocene carbon dynamics in a large boreal peatland complex, southern Finland, Quaternary Science Reviews, 142, 1–15, https://doi.org/10.1016/j.quascirev.2016.04.013, 2016.

Mauder, M. and Foken, T.: Documentation and Instruction Manual of the Eddy Covariance Software Package TK2, Arbeitsergebnisse, 2004.

Oksanen, J., Blanchet, F. G., Kindt, R., Legendre, P., Minchin, P., O'Hara, B., Simpson, G., Solymos, P., Stevens, H., and Wagner, H.: Vegan: Community Ecology Package, R Package Version 2.2-1, 2, 1–2, 2015.

Reichstein, M., Falge, E., Baldocchi, D., Papale, D., Aubinet, M., Berbigier, P., Buchmann, N., Gilmanov, T., Granier, A., Grünwald, T., Havránková, K., Ilvesniemi, H., Janous, D., Knohl, A., Laurila, T., Lohila, A., Loustau, D., Matteucci, G., and Valentini, R.: On the Separation of Net Ecosystem Exchange into Assimilation and Ecosystem Respiration: Review and Improved Algorithm, Global Change Biology, 11, 1424–1439, https://doi.org/10.1111/j.1365-2486.2005.001002.x, 2005.

Rinne, J., Riutta, T., Pihlatie, M., Aurela, M., Haapanala, S., Tuovinen, J.-P., Tuittila, E.-S., and Vesala, T.: Annual cycle of methane emission from a boreal fen measured by the eddy covariance technique, Tellus B: Chemical and Physical Meteorology, 59, 2007.

Rinne, J., Tuittila, E.-S., Peltola, O., Li, X., Raivonen, M., Alekseychik, P., Haapanala, S., Pihlatie, M., Aurela, M., Mammarella, I., and Vesala, T.: Temporal Variation of Ecosystem Scale Methane Emission From a Boreal Fen in Relation to Temperature, Water Table Position, and Carbon Dioxide Fluxes, Global Biogeochem. Cycles, 32, 1087–1106, https://doi.org/10.1029/2017GB005747, 2018.

Rinne, J., Tuovinen, J.-P., Klemedtsson, L., Aurela, M., Holst, J., Lohila, A., Weslien, P., Vestin, P., Łakomiec, P., Peichl, M., Tuittila, E.-S., Heiskanen, L., Laurila, T., Li, X., Alekseychik, P., Mammarella, I., Ström, L., Crill, P., and Nilsson, M. B.: Effect of the 2018 European drought on methane and carbon dioxide exchange of northern mire ecosystems, Phil. Trans. R. Soc. B, 375, 20190517, https://doi.org/10.1098/rstb.2019.0517, 2020.

https://doi.org/10.5194/egusphere-2026-3323
Preprint. Discussion started: 24 June 2026

Riutta, T., Laine, J., Aurela, M., Rinne, J., Vesala, T., Laurila, T., Haapanala, S., Pihlatie, M., and Tuittila, E.-S.: Spatial variation in plant community functions regulates carbon gas dynamics in a boreal fen ecosystem, Tellus B: Chemical and Physical Meteorology, 59, 2007.

Rydin, H., Jeglum, J. K., and Bennett, K. D.: The biology of peatlands, 2nd ed., Oxford University Press, Oxford, 382 pp., 2013.

Saarnio, S., Winiwarter, W., and Leitão, J.: Methane release from wetlands and watercourses in Europe, Atmospheric Environment, 43, 1421–1429, https://doi.org/10.1016/j.atmosenv.2008.04.007, 2009.

Särkelä, K., Vesala, T., Christensen, T. R., Cohen, J., Kübert, A., Li, X., Marttila, H., Pulliainen, J., Tuittila, E.-S., and López-Blanco, E.: Ecosystem respiration during snowmelt and soil thaw leads to a rare annual CO_2 net loss in a boreal fen, EGUsphere, 1–24, https://doi.org/10.5194/egusphere-2025-5778, 2025.

Saunois, M., Martinez, A., Poulter, B., Zhang, Z., Raymond, P. A., Regnier, P., Canadell, J. G., Jackson, R. B., Patra, P. K., Bousquet, P., Ciais, P., Dlugokencky, E. J., Lan, X., Allen, G. H., Bastviken, D., Beerling, D. J., Belikov, D. A., Blake, D. R., Castaldi, S., Crippa, M., Deemer, B. R., Dennison, F., Etiope, G., Gedney, N., Höglund-Isaksson, L., Holgerson, M. A., Hopcroft, P. O., Hugelius, G., Ito, A., Jain, A. K., Janardanan, R., Johnson, M. S., Kleinen, T., Krummel, P. B., Lauerwald, R., Li, T., Liu, X., McDonald, K. C., Melton, J. R., Mühle, J., Müller, J., Murguia-Flores, F., Niwa, Y., Noce, S., Pan, S., Parker, R. J., Peng, C., Ramonet, M., Riley, W. J., Rocher-Ros, G., Rosentreter, J. A., Sasakawa, M., Segers, A., Smith, S. J., Stanley, E. H., Thanwerdas, J., Tian, H., Tsuruta, A., Tubiello, F. N., Weber, T. S., van der Werf, G. R., Worthy, D. E. J., Xi, Y., Yoshida, Y., Zhang, W., Zheng, B., Zhu, Q., Zhu, Q., and Zhuang, Q.: Global Methane Budget 2000–2020, Earth System Science Data, 17, 1873–1958, https://doi.org/10.5194/essd-17-1873-2025, 2025.

Sulman, B. N., Desai, A. R., Saliendra, N. Z., Lafleur, P. M., Flanagan, L. B., Sonnentag, O., Mackay, D. S., Barr, A. G., and van der Kamp, G.: CO2 fluxes at northern fens and bogs have opposite responses to inter-annual fluctuations in water table, Geophysical Research Letters, 37, https://doi.org/10.1029/2010GL044018, 2010.

Tahvanainen, T.: Abrupt ombrotrophication of a boreal aapa mire triggered by hydrological disturbance in the catchment, Journal of Ecology, 99, 404–415, https://doi.org/10.1111/j.1365-2745.2010.01778.x, 2011.

Turetsky, M. R., Kotowska, A., Bubier, J., Dise, N. B., Crill, P., Hornibrook, E. R. C., Minkkinen, K., Moore, T. R., Myers-Smith, I. H., Nykänen, H., Olefeldt, D., Rinne, J., Saarnio, S., Shurpali, N., Tuittila, E.-S., Waddington, J. M., White, J. R., Wickland, K. P., and Wilmking, M.: A synthesis of methane emissions from 71 northern, temperate, and subtropical wetlands, Global Change Biology, 20, 2183–2197, https://doi.org/10.1111/gcb.12580, 2014.

Turner, J. C., Moorberg, C. J., Wong, A., Shea, K., Waldrop, M. P., Turetsky, M. R., and Neumann, R. B.: Getting to the Root of Plant-Mediated Methane Emissions and Oxidation in a Thermokarst Bog, Journal of Geophysical Research: Biogeosciences, 125, e2020JG005825, https://doi.org/10.1029/2020JG005825, 2020.

Turunen, J., Tomppo, E., Tolonen, K., and Reinikainen, A.: Estimating carbon accumulation rates of undrained mires in Finland–application to boreal and subarctic regions, The Holocene, 12, 69–80, https://doi.org/10.1191/0959683602hl522rp, 2002.

Vekuri, H., Tuovinen, J.-P., Kulmala, L., Papale, D., Kolari, P., Aurela, M., Laurila, T., Liski, J., and Lohila, A.: A widely-used eddy covariance gap-filling method creates systematic bias in carbon balance estimates, Sci Rep, 13, 1720, https://doi.org/10.1038/s41598-023-28827-2, 2023.

https://doi.org/10.5194/egusphere-2026-3323
Preprint. Discussion started: 24 June 2026

Webb, E. K., Pearman, G. I., and Leuning, R.: Correction of flux measurements for density effects due to heat and water vapour transfer, Quarterly Journal of the Royal Meteorological Society, 106, 85–100, https://doi.org/10.1002/qj.49710644707, 1980.

Webster, K. L., Bhatti, J. S., Thompson, D. K., Nelson, S. A., Shaw, C. H., Bona, K. A., Hayne, S. L., and Kurz, W. A.: Spatially-integrated estimates of net ecosystem exchange and methane fluxes from Canadian peatlands, Carbon Balance Manage, 13, 16, https://doi.org/10.1186/s13021-018-0105-5, 2018.

Wuebbles, D. J. and Hayhoe, K.: Atmospheric methane and global change, Earth-Science Reviews, 57, 177–210, https://doi.org/10.1016/S0012-8252(01)00062-9, 2002.

Ye, R., Jin, Q., Bohannan, B., Keller, J. K., McAllister, S. A., and Bridgham, S. D.: pH controls over anaerobic carbon mineralization, the efficiency of methane production, and methanogenic pathways in peatlands across an ombrotrophic–minerotrophic gradient, Soil Biology and Biochemistry, 54, 36–47, https://doi.org/10.1016/j.soilbio.2012.05.015, 2012.

Yu, Z. C.: Northern peatland carbon stocks and dynamics: a review, Biogeosciences, 9, 4071–4085, https://doi.org/10.5194/bg-9-4071-2012, 2012.

Zhang, H., Tuittila, E., Korrensalo, A., Laine, A. M., Uljas, S., Welti, N., Kerttula, J., Maljanen, M., Elliott, D., Vesala, T., and Lohila, A.: Methane production and oxidation potentials along a fen-bog gradient from southern boreal to subarctic peatlands in Finland, Global Change Biology, 27, 4449–4464, https://doi.org/10.1111/gcb.15740, 2021.

Zhao, Y., Feng, X., Pihlatie, M., Putkinen, A., Männikkö, M., Wang, H., Liu, C., Aurela, M., and Li, X.: Warming enhances soil carbon accumulation in boreal Sphagnum peatlands, Nat Ecol Evol, 10, 496–511, https://doi.org/10.1038/s41559-026-02982-x, 2026.